Journal of Colloid and Interface Science 512 (2018) 172–189

Contents lists available at ScienceDirect

Journal of Colloid and Interface Science

journal homepage: www.elsevier.com/locate/jcis

Regular Article

Catalytic decomposition of 2-chlorophenol using an ultrasonic-assisted Fe_3O_4–TiO_2@MWCNT system: Influence factors, pathway and mechanism study

Sina Dobaradaran [a,b,c], Ramin Nabizadeh Nodehi [d], Kamyar Yaghmaeian [d], Jalil Jaafari [e], Maryam Hazrati Niari [f], Arvind Kumar Bharti [g], Shilpi Agarwal [g], Vinod Kumar Gupta [g,i,*], Ali Azari [h,d,*], Nabi Shariatifar [d]

[a] The Persian Gulf Marine Biotechnology Research Center, Bushehr University of Medical Sciences, Bushehr, Iran
[b] Department of Environmental Health Engineering, Faculty of Health, Bushehr University of Medical Sciences, Bushehr, Iran
[c] Systems Environmental Health, Oil, Gas and Energy Research Center, Bushehr University of Medical Sciences, Bushehr, Iran
[d] Department of Environmental Health Engineering, School of Public Health, Tehran University of Medical Sciences, Tehran, Iran
[e] School of Health, Guilan University of Medical Sciences, Rasht, Iran
[f] Department of Environmental Health Engineering, School of Public Health, Jundishapur University of Medical Sciences, Ahvaz, Iran
[g] Department of Applied Chemistry, University of Johannesburg, Johannesburg, South Africa
[h] Department of Environmental Health Engineering, School of Public Health, Kashan University of Medical Sciences, Kashan, Iran
[i] Department of Biological Sciences, Faculty of Science, King Abdulaziz University, Jeddah, Saudi Arabia

GRAPHICAL ABSTRACT

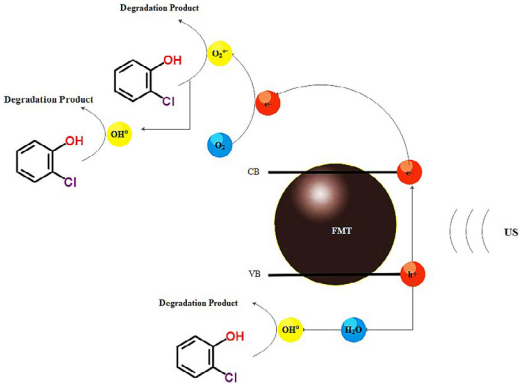

ARTICLE INFO

Article history:
Received 21 August 2017
Revised 4 October 2017
Accepted 4 October 2017
Available online 12 October 2017

Keywords:
Fe_3O_4–TiO_2@MWCNT nanocomposite

ABSTRACT

As a reusable sonocatalyst, magnetically separable Fe_3O_4–TiO_2@MWCNT (FMT) was synthesized by an ultrasound-assisted wet impregnation method and was evaluated in the removal of 2-chlorophenol (2CP). Physical and chemical properties of the catalyst composite materials were investigated by all catalysts were systematically characterized using Transmission Electron Microscopy (TEM), X-ray diffraction (XRD), Scanning Electron Microscopy (SEM), X-ray Photoelectron Spectroscopy (XPS), Energy Dispersive X-ray Analysis (EDX), Dynamic light scattering (DLS), and N_2-physisorption. The efficiency and kinetics of 2CP removal by FMT-assisted sonocatalysis (FMT-US) was systematically investigated under various operational parameters i.e. pH, FMT and 2CP concentration, temperature and ultrasonic

* Corresponding authors at: Department of Applied Chemistry, University of Johannesburg, Johannesburg, South Africa (V.K. Gupta); Department of Environmental Health Engineering, School of Health, Tehran University of Medical Sciences, P. O. Box: 6446-14155, Tehran 1471613151, Iran (A. Azari).
E-mail addresses: s.dobaradaran@bpums.ac.ir (S. Dobaradaran), rnabizadeh@tums.ac.ir (R.N. Nodehi), k_yaghmaeian@yahoo.com (K. Yaghmaeian), jalil.jaafari@yahoo.com (J. Jaafari), hazrati.m@ajums.ac.ir (M.H. Niari), vinodfcy@gmail.com, vinodg@uj.ac.za (V.K. Gupta), Azari.hjh@gmail.com (A. Azari).

https://doi.org/10.1016/j.jcis.2017.10.015

Heterogeneous catalysis
2-clorophenol
Ultrasonic irradiation

power. The results indicated that 0.4 g L^{-1} FMT dosage, pH 5, temperature of 35 °C as well as 50 w ultrasound power are the most favorable conditions for the degradation of the 2CP. Furthermore, both of the superoxide and hydroxyl radicals were produced in the reaction, however, superoxide radicals were assumed to be the dominating reactive species for the 2CP degradation, according to the scavenging tests and electron paramagnetic resonance tests. Moreover, the FMT catalyst exhibited a high reusability and stability in the US/FMT system during the five repetitive experiments. The intermediate products were identified by GC–MS, thereby a possible degradation pathway is proposed. The chemical oxygen demand (COD) and corresponding total organic carbon (TOC) removal efficiencies were 64.9% and 56.7%, respectively. Finally, toxicity tests showed that the toxicity of the solution increased during the first 5 min and then decreased significantly with the progress of the oxidation. The mechanisms of ultrasound irritation enhanced FMT activation were also proposed.

1. Introduction

Chlorinated phenolic compounds i.e. 2-Chlorophenol (2CP), 4-chlorophenol (4-CP), 2,4-dichlorophenol (2,4-DCP) and pentachlorophenol (PCP) have been widely known to have severe detrimental effects on aquatic ecosystem and human health [1]. In the chlorinated phenolic families, 2CP due to high toxicity, carcinogenic character, persistence in the environment, and low biodegradability have been listed among priority pollutants by the United States Environmental Protection Agency [2]. The main routes of entry of 2CP to the aquatic system are via industrial operations (such as the bleaching of pulp with chlorine, hydrolysis of chlorinated herbicides and oil refining) or formed as a result of the chlorination of humic matter during the chlorination of municipal drinking water [3,4]. They may also be introduced into the environment during their manufacture and use or through degradation of other chemicals (e.g., phenoxyakanoic acids) [5]. 2CP exposure is associated with various health and ecotoxicological risks to the human and aquatic wild life; even very low concentrations have resulted in harmful effects on the human endocrine system and aquatic wild life reproduction [6]. Hence, the removal of 2CP from wastewater represents an emerging environmental concern. A wastewater stream containing 2CP over 200 mg L^{-1} may not be treated effectively by direct biological methods [7], therefore decomposition of 2CP has been examined extensively by photocatalytic [8], electrocatalytic [9], Fenton's oxidation [10] and more recently, sonochemical methods [11]. Among the mentioned treatment technologies, TiO_2 photocatalysis because of its good activity, chemical stability, commercial availability and inexpensiveness has well-known as a promising technology for organic contamination treatment [12]. However, the separation and recovery of photo catalyst are difficult, which limit the application of TiO_2 slurry reactor in practical application [13]. The recent studies have been focused on the immobilizing TiO_2 onto magnetic substrates i.e. Fe_3O_4 NPs, which provide a very convenient approach for the separation and recycling of the photocatalyst [14]. However, Fe_3O_4 nanoparticles (NPs) are susceptible to air oxidation. Moreover, directly introducing Fe_3O_4 NPs as the core of the Fe_3O_4@TiO_2 nanostructure would produce photo dissolution problems [15]. Many researches indicated that the photodissolution problem could be prevented by introducing a passivation layer between the Fe_3O_4 core and the TiO_2 shell [16]. MWCNTs are 1D carbon-based ideal molecules with a nano cylindrical structure, which can conduct electricity at room temperature with essentially no resistance (ballistic transport) [17]. While the electrons formed by UV irradiation migrate to the surface of the MWCNTs, they are easily transported into the conduction band (CB) of TiO_2 which is bound with them [17,18]. Hence, the increased amount of generated photoelectrons can decrease the high rate of electron/hole pair recombination, which otherwise reduces the quantum yield of the TiO_2 process [19]. Besides, the use of TiO_2 without the worry about agglomeration at higher concentration, adsorption of intermediate products that are produce after the reaction, and concentrate the pollutants near TiO_2 particles to continue the degradation process is another important point about MWCNTs [20,21]. When this catalyst is used in industrial waste treatment the catalyst cannot absorb the ultraviolet radiation properly due to the dark nature of the industrial effluent [22]. This problem can sometimes be overcome by using high power ultraviolet light, which increases both the energy consumption and equipment's price [22]. A good alternative to ultraviolet excitation is ultrasonic irradiation. The process catalyzed by ultrasound is named sonocatalysis. The ultrasound effect on molecules is related to cavitation, nucleation, growth and implosion of microbubbles that trap steam/gas [22,23]. These microbubbles produce areas of high pressure, which lead to water dissociation and formation of OH radicals. These radicals are responsible for the degradation process [24,25]. The ultrasound irradiation induces electrons' movement on the TiO_2 crystal network, increasing the electron-hole pair number and increasing the OH radical concentration in the reaction medium as well [26]. Moreover, radial ultrasound may disperse the aggregated catalyst particles, thereby increasing active surface area. Furthermore, radial ultrasound is also beneficial to the activation of the reused photocatalysis [27]. Although many studies have addressed this issue that combining ultrasound with TiO_2 can enhance the efficiency of semiconductor mediated degradation of organic contaminants synergistically, but designed magnetic core-shell sonocatalyst possesses a uniform size, good structural stability, high surface area, excellent magnetic separation, and remarkable sonocatalytic performance still remains as a challenge. According to the above mentioned, the purpose of this report was centered to combination the advantages of MWCNTs and Fe_3O_4 to design an effective catalyst, characterization of prepared catalysts by XRD, EDX, SEM, PDI, DLS, XPS, VSM and TEM techniques, evaluation the catalytic activity, reusability and stability of catalysts in FMT-US system, investigation the reaction mechanisms and degradation pathway, determination the amount of iron and titanium leaching during the degradation process and finally toxicity assessment.

2. Materials and methods

2.1.Reagents

Reagents and chemicals used for the study were given in Supplementary material S1.

2.2. Synthesis of catalysts

Preparation of Fe_3O_4 by co-precipitation method, TiO_2 by sol-gel route, magnetic Fe_3O_4–TiO_2 via a sonochemical route, and MWCNT-TiO_2 nano-composite using the sol–gel method was

applied to the present work are given separately in Supplementary material S1.

2.2.1. Preparation of Fe_3O_4- MWCNT-TiO_2 (FMT) nanocomposites

Magnetic Heterogeneous Fe_3O_4–TiO_2@MWCNT catalyst was prepared using ultrasound-assisted wet impregnation method is as follows: Different wt% of Fe (III) chloride and predetermined amount of MWCNT-TiO_2 nano-composite were added to 100 mL of deionized water under continuous stirring for 24 h at room temperature. The resulting mixture then sonicated for 30 min in the ultrasonic cleaning bath (KQ-300DE, 40 kHz, 300 W). After mixing, the solution was evaporated using water bath at 100 °C under continuous stirring. The obtained catalysts were dried for 48 h at 100 °C and then calcined at 500 °C for 4 h. Subsequently obtained catalysts were named according to the different Fe loading onto TiO_2: Fe_3O_4 i.e. TiO_2 - Fe_3O_4 (1:1) TiO_2 - Fe_3O_4 (9:1).

2.3. Characterization and analytical method

All catalysts were systematically characterized using Transmission Electron Microscopy (TEM), X-ray diffraction (XRD), Scanning Electron Microscopy (SEM), X-ray Photoelectron Spectroscopy (XPS), Energy Dispersive X-ray Analysis (EDX), Dynamic light scattering (DLS), vibrating sample magnetometer (VSM) and N_2-physisorption (see Supplementary material S1). The concentrations of 2CP during degradation were analyzed by an Agilent 1100 Series HPLC system (Agilent Technologies, Santa Clara, CA) equipped with a diode array detector and reverse phase column (150 × 4.6 mm, 5 μm particle, Zorbax 300SB-C18, Agilent, USA) under the following conditions: the mobile phase was an 80:20 (v/v) mixture of methanol and water at 1.0 mL min^{-1}; injection volume was 20 μL; detection wavelength was set at 230 nm and column temperature 30 °C; retention time, 0.8 min. The intermediates generated during the degradation of 2CP were detected by an Agilent 6890 gas chromatograph with a 30-m–0.25-mm HP-5MS capillary column coupled with an Agilent 5973 mass spectrometer (USA). Helium, as carrier gas, was fed into the instrument with a constant flow rate of 1 mL min^{-1}. The initial temperature of the oven was set to 40 °C for 1 min. Then, it was increased to 300 °C at increasing rate of 5 °C/min and maintained for 3 min. The Fe and Ti ion concentrations were measured using an inductively coupled plasma mass spectrophotometer (ICP-MS; Agilent 7500, Ce, Japan) and extent of mineralization during degradation evaluated by total organic carbon (TOC) content using a TOC- 5000A analyzer (Shimadzu, Japan). The chemical oxygen demand (COD) was determined (Merck Spectroquant TR320) by a closed reflux colorimetric method according to Standard Methods for the Examination of Water and Wastewater (APHA, A., WPCF 1985).

2.4. Reaction procedure: Sonocatalytic and photocatalytic activities

The catalytic activities of the FMT composites were determined by the degradation and mineralization of 2CP in aqueous solution. The catalysts (0.2 g) were suspended in 200 mL of 2CP solution with a desired concentration in a glass vessel. The 2CP solutions and NPs were stirred magnetically in dark for 30 min prior to ultrasonication or UV–visible light to ensure that the adsorption/desorption equilibrium of the substrate on the catalyst was achieved as well as effect of adsorption during sonocatalysis or photocatalysis was eliminated. For the degradation process of 2CP, a plastic container (diameter = 20 cm, height = 10 cm) filled with ice was used to adjustment a temperature environment at around predetermined amount. A schematic diagram of the sonocatalytic is shown in Fig. 1S. It consists of four parts: an ultrasonic generator, constant temperature controller, ice water bath, and reactor. The initial pH of the 2CP solutions was adjusted to 3–11 with HCl (0.1 mol L^{-1}) and NaOH (0.1 mol L^{-1}) using pH meter (Jenway 3510). Sonocatalytic degradation was tested using the FMT catalysts with ultrasonic generators operated at power of 25–100 W L^{-1}, respectively. The reactions were carried out in an open cylindrical stainless glass vessel. The ultrasonic irradiation of the reactor was done for definite interval of time. After desired time interval of ultrasonic irradiation and the removal of the dispersed powders through external magnet, samples were withdrawn from the reactor, and clean transparent solution was analyzed using a HPLC. In case of photocatalysis, the prepared suspended solution was placed in UV–visible chamber (125 W, 198.4 mW S^{-2}) under stirring, which disperse the NPs in the solution. After desired time interval of UV–visible irradiation, samples were withdrawn from the reactor, and changes 2CP concentration were measured. The effects of the dimethyl sulfoxide (DMSO), carbonate, sulphate and chloride as common inorganic anions on the degradation performance were investigated by separately adding of their salt into the reaction solution.

Meanwhile the effect of 1,4-benzoquinone and tert-butanol as a scavenger on the sonocatalytic degradation was investigated. The sonocatalytic and photocatalytic activities of samples in terms of 2CP degradation was reported by using the following equation:

$$\textbf{Degradation efficiency}(\%) = \frac{\mathbf{C_0} - \mathbf{C_f}}{\mathbf{C_0}} \times 100 \quad (1)$$

where $\mathbf{C_0}$ and $\mathbf{C_f}$ is the initial and final absorbance of the 2CP solutions after degradation. The kinetic studies for sonocatalysis and photocatalysis systems were carried out in amber flasks after optimization of process condition. The catalytic degradation followed the first-order reaction (Eq. (2)), where $\mathbf{k_{app}}$ is the apparent-first-order reaction rate constant (min^{-1}), $\mathbf{C_0}$ is the initial concentration in the bulk solution (mg L^{-1}) and **t** is the reaction time (min):

$$\ln\left(\frac{\mathbf{C_0}}{\mathbf{C_f}}\right) = \mathbf{k_{app}} \times \mathbf{t} \quad (2)$$

The degree of mineralization was evaluated by monitoring the reduction in organic carbon of the samples using a TOC and COD analyzes

3. Results and discussion

3.1. Characterization of nanocomposites

3.1.1. XRD analysis

The XRD technique (Fig. 1a) was used to determine the crystallographic structure of the MWCNTs-TiO_2(a) and (b) FMT. For the MWCNTs-TiO_2 composite, nine distinctive peaks located at 2θ = 25.4°, 37.9°, 48.1°, 54.2°, 55.1°, 62.8°, 69.1°, 70.3° and 75.4°, which correspond to the (1 0 1), (0 0 4), (2 0 0), (1 0 5), (2 1 1), (2 0 4), (1 1 6), (2 2 0) and (2 1 5) reflections ofthe anatase TiO_2, respectively, indicating that the titanium dioxide in the structure of MWCNTs-TiO_2 existed as the anatase (JCPDS: No. 21-1272). The characteristic peaks of the MWCNTs could be identified in both of the patterns of the composite samples at 2θ of about 26° and 43° are assigned to (0 0 2) and (1 1 0) planes, which indicates that the MWCNT component in the nanocomposite is in amorphous state. From the XRD results of the FMT composites, all the diffraction peaks of TiO_2 were maintained after the Fe_3O_4 deposition, which indicated that the effects of Fe_3O_4 on crystal structure of the FMT nanoparticles were negligible and (b) TiO_2 also existed in the anatase phase in it. Meanwhile, the new prominent peaks appeared at of 35.6°, 46.1°, 56.8°, and 63.8° were attribute to the reflections from the (1 0 2), (1 0 3), (1 1 2), and (2 0 3) planes of the cubic spinel structure magnetite, respectively (JCPDS: No. 19-0629); which

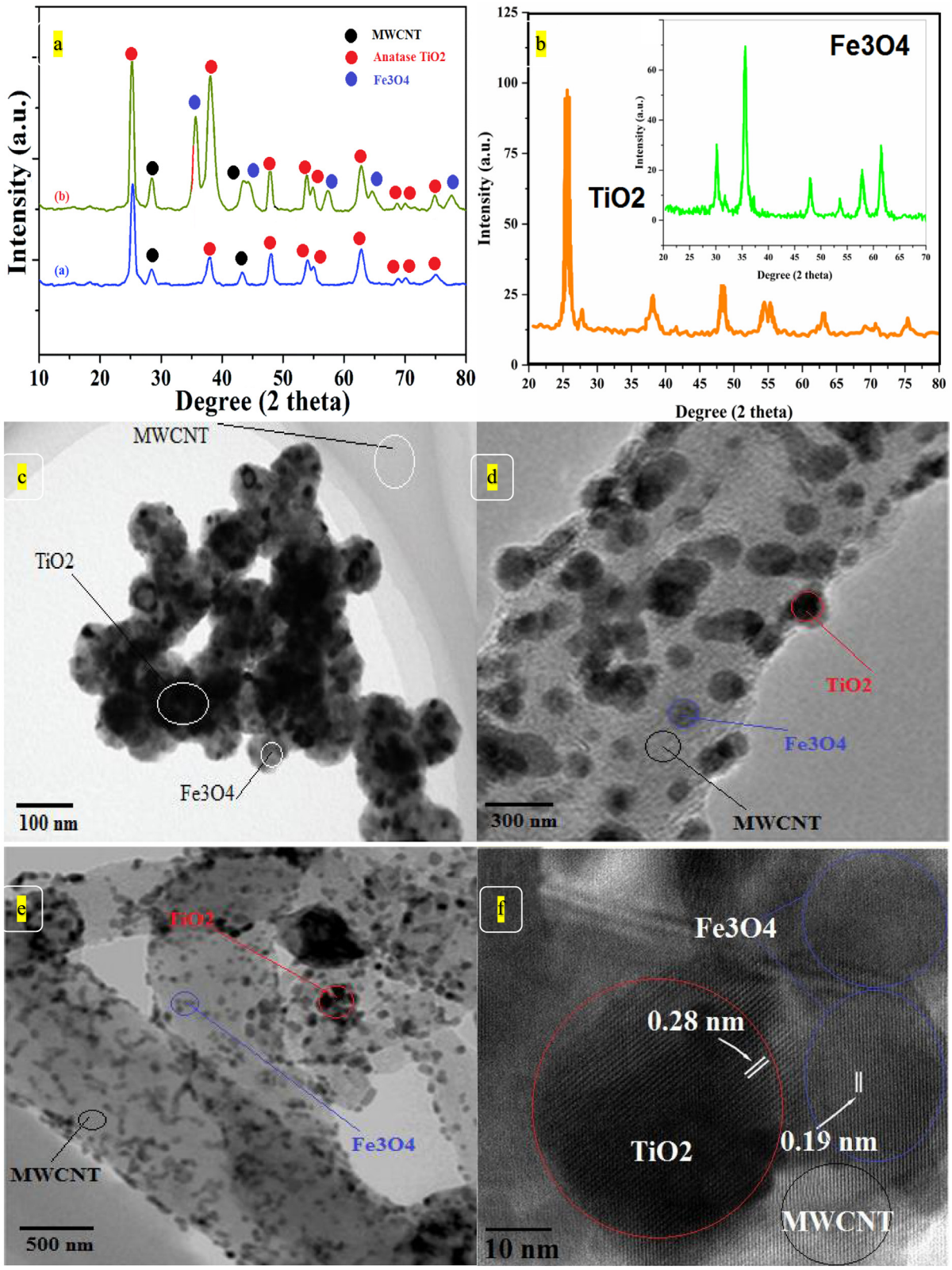

Fig. 1. XRD spectra of MWCNTs-TiO_2 and FMT (a), XRD spectra of pure TiO_2 and Fe_3O_4 (b), TEM images of FMT (c, d and e), HRTEM images of the FMT (f).

are similar as the XRD features of the commercial Fe_3O_4 powder. The broad nature peak of the deposited TiO_2 is an indication of the small crystallite size. The mean size of a single TiO_2 crystallite, can also be determined from the broadening of corresponding X-ray diffraction peaks by using Scherrer's formula:

$$\mathbf{D} = \frac{\mathbf{K}\lambda}{\beta \cos\theta} \tag{3}$$

where λ is the wavelength of the X-ray radiation (λ = 0.15418 nm), K is the Scherrer constant (K = 0.89), θ is the angle of the X-ray

diffraction peak and β is the full-width at half-maximum (FWHM) of the (1 0 1) plane (here β = 0.68°). The estimated crystallite size of TiO_2 was about 12.3 nm. XRD patterns of pure TiO_2 and Fe_3O_4 nanoparticles are also shown in the Fig. 1b. As shown all the reflection peaks for pure TiO_2 and Fe_3O_4 are in good agreement with the results obtained from FMT composites reflection. (Fig. 1a).

3.1.2. TEM analysis

To examine the uniformity and structural design of the FMT composites, the samples were investigated by HR-TEM. Fig. 1c confirmed the TiO_2 nanoparticles are heterogeneously distributed on the surface of MWCNTs. Similarly, Fig. 1d,e shows HR-TEM images for FMT in various magnification. The result revealed that TiO_2 nanoparticles are well dispersed on the wall support with a few agglomerations observed (big grains). TiO_2 nanoparticles in composite structure was mainly spherical (dark spots) with a mean diameter of around 12.9 nm, whereas the diameter of the MWCNTs was found to be 20–45 nm. It is in agreement with the above XRD results. A high-magnification HRTEM was used to further investigate the structure of the FMT sample. This revealed that the prepared samples were well crystallized, as evidenced by well-defined lattice fringes. The small crystallite size and the well crystallized structure contributed to the efficient sono and photo catalytic property of hybrid catalyst, which was confirmed by the subsequent sono/photo catalytic activity studies of the FMT nanocomposites [28]. From Fig. 1f, can be observed that TiO_2 is attached to the Fe_3O_4 nanocrystal, and that the interplanar distance of that nanoparticle is about 0.19 nm, revealing the crystalline nature of the nanocrystal; the interplanar distance of the Fe_3O_4 microspheres is about 0.28 nm and corresponds to its (3 1 1) plane. Generally, the HRTEM analysis confirmed that both Fe_3O_4 and TiO_2 coexisted in the resulting MWCNTs matrix. Furthermore, an interconnected nanoparticle morphology (Fig. 1f), indicates that a Fe_3O_4–TiO_2 nanocrystal heterojunction is formed in the composite.

3.1.3. PDI and DLS analysis

The hydrodynamic diameter (average size distribution) and polydispersity index (PDI) of the synthesized composites in the terms of various TiO_2:Fe_3O_4 ratio content was estimated by Dynamic Light Scattering (DLS) and Particle Size Analyzer (PSA). Particle size analysis of FMT composites showed that the size and polydispersity of the synthesized composite at TiO_2:Fe_3O_4 ratio of 5:1 is smaller than that other one (Fig. 2S). In fact, among synthesized composite, FMT with an TiO_2:Fe_3O_4 ratio of 5:1 showed a smaller size (12 ± 0.2 nm) with a lower PDI (0.22), indicating that slightly higher TiO_2: Fe_3O_4 ratios were required for smaller complexes (Table 1S). Additionally, FMT composites formed <13.1 nm and no significant differences among PDI of synthesized nanoparticles in all TiO_2:Fe_3O_4 ratio confirmed the monodispersity of synthesized NPs [29].

3.1.4. SEM and EDX analysis

The morphology and microstructure of the hybrid composites have been elucidated by electron microscopy. The SEM images of the FMT composites at six different magnifications are shown in Fig. 2. It can clearly observe that the MWCNTs were heterogeneously decorated by well-dispersed particles with only a few TiO_2 aggregates. The porous structure of FMT composites as well as non-uniformly dispersed of TiO_2 on the entire surface of the prepared composite was observed in Fig. 2b–f. Indeed, at a closer magnification, it appears that nanotubes walls are almost entirely covered by Fe_3O_4 and TiO_2. The rough structure of FMT and well distribution of TiO_2 in the structure of catalyst leads to enhance mass-transfer rate of 2CP on composites surface. Fig. 3S represents the EDX analysis of Fe_3O_4 and TiO_2 decorated onto the MWCNT. Ti, Fe, O and C elements are observed in the final composition. Ti (35.72 wt%) and Fe (7.5 wt%) are the main element of Fe_3O_4 and TiO_2, respectively and C (39.23 wt%) peak belongs to the MWCNT. O (17.55 wt%) peak belong to oxidized site onto the MWCNT, Fe_3O_4 and TiO_2 as well (Table 2S). Interesting, by EDX numerical analysis, the Ti: Fe molecular ratio was obtained to be about 4.763 which is close to the best FMT structure in PDI and DLS experiments (Section 3.1.3).

3.1.5. XPS analysis

XPS were further used to elucidate the detailed surface chemical compositions of the Fe_3O_4 and TiO_2 nanoparticles immobilized on MWCNT. From the survey spectrum of FMT composites, can confirm the presence of Fe and Ti over the surface of MWCNT. In FMT composites spectrum a peak appears at 458.8 eV assigned to the photoelectrons originating from the Ti 2p energy level, which responds to the Ti element in the hybrid catalyst. Moreover, binding energy peaks observed at 284.8 eV, 530 eV and 710.5 eV indicate the presence of C 1s, O 1s and Fe 2p in composite structure. The peaks observed for Fe is small than C and Ti due to its low concentration. Fig. 3b showed the XPS spectra of O1s core level of the samples. The binding energy peak observed at 531.2 eV could be attributed to —OH on the surface and Ti—O—Ti. Two peaks at 529.6 and 532.7 eV as shown in Fig. 3b, which were assigned to Fe—O and Fe—O—H, respectively [30,31]. Fig. 3c showed the XPS of C1s of the samples. Three peaks at 283.8, 285.1 and 287.5 eV can be identified, respectively. The strong peak at 283.8 eV was assigned to C—C, arising from the incomplete burning of organic compounds, and the adventitious carbon absorbed on the surface of the sample. In addition, significant peaks observed at 285.1 and 287.5 eV were assigned to C—O and C = O bonds. Besides, the peak observed for Fe2p confirms formation Ti—O—Fe bonds due to the substitution of Ti^{2+} by Fe^{3+} in FMT composites. To investigate the formation of Fe^0 (NZVI) during the degradation process, XPS spectra of the recovered samples after reaction was analyzed. Like as fresh catalyst, binding energy peaks observed at • 710.5 eV indicate the presence of Fe 2p in composite structure. The intensity of Fe2p XPS spectrum was very weak (Fig. 3e), corresponding to the low Fe content. As shown in Fig. 3d, Fe atoms were divided into Fe^{2+} and Fe^{3+}. The Fe^{3+}/Fe^{2+} ratio of FMT was 1.9 after reaction. The starting Fe^{3+}/Fe^{2+} ratio of fresh materials was 1.88, indicating that Fe^{2+} was slightly oxidized during the degradation process. Furthermore, according to the previous studies, in the presence of iron in the reduced form (Fe^0), clear peaks be created between 705 and 707.5 eV. There is no courier observed before and after degradation in mention eV, which confirm the above results.

3.1.6. VSM analysis

The magnetic property of prepared Fe_3O_4 and FMT composites is investigated with vibrating sample magnetometer at room temperature. From the magnetization-hysteresis loops of samples (Fig. 4S) can be found magnetic saturation value of the FMT composites is lower than that of the pristine Fe_3O_4 (~43 emu/g < ~80.8 emu/g). The decrease in saturation magnetization is mainly due to the existence of non-magnetic TiO_2 and MWCNT on the surface of the nanocomposites texture. In other side, the coercivity (Hc) and remanent magnetization (Mr) of the nanocomposites are close to zero, representing that hybrid catalyst exhibits superparamagnetic properties at room temperature. Superparamagnetic properties are very important to the recyclable sono and/or photo catalytic properties of a hybrid catalyst. With superparamagnetic properties, the magnetic composites can be recovered efficiently by imparting an external magnetic field. The Fig. 4S **(inset)** is the image of FMT separation from aqueous solution by

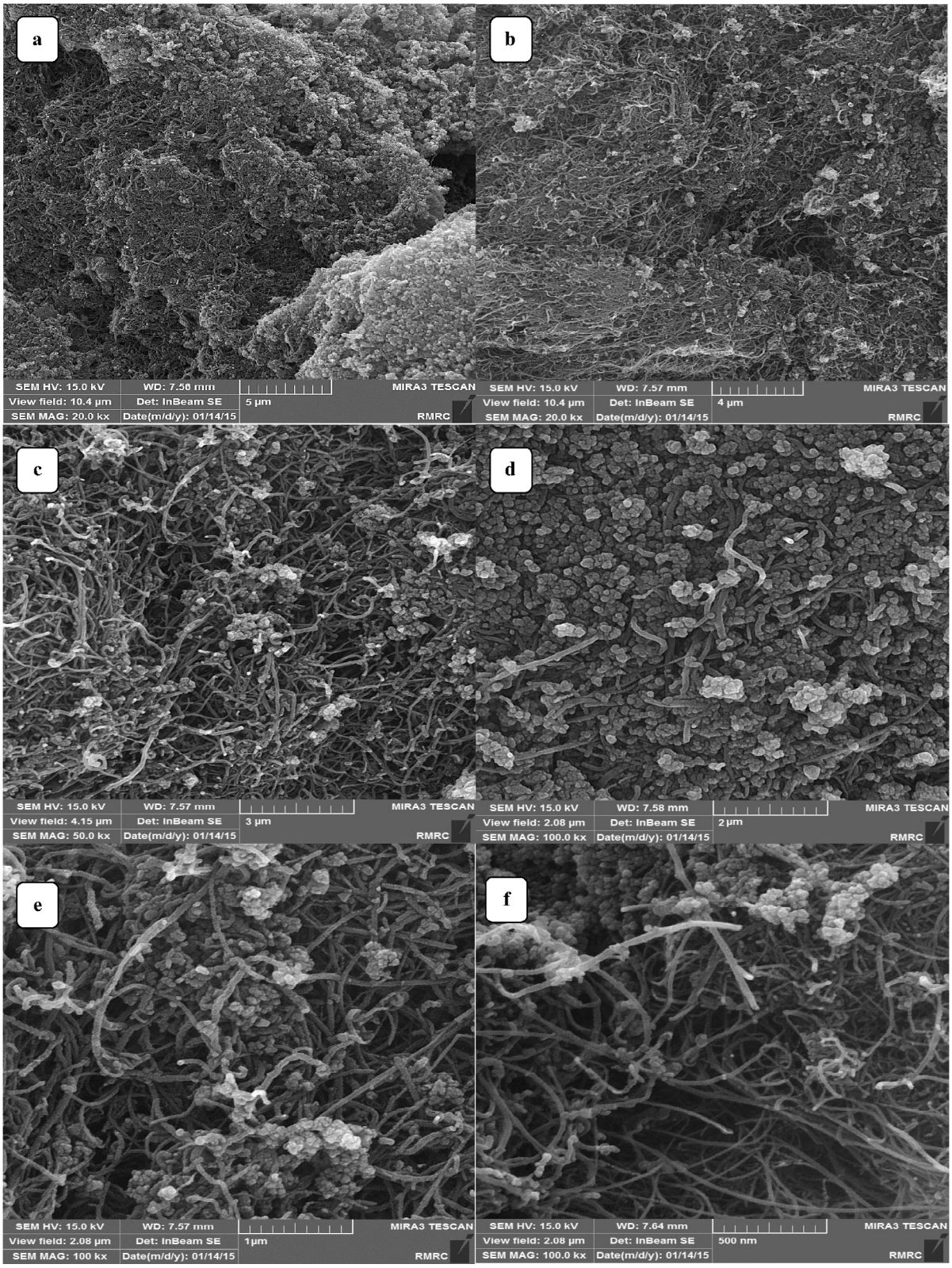

Fig. 2. SEM image of a FMT at six different magnifications.

an external magnetic field. In fact, the magnetic catalystis recycled easily by attracting towards the magnet located in right-hand side of sample vials over a 10 s, demonstrating the high magnetic sensitivity of synthesized magnetic hybrid catalyst

3.1.7. Dispersion analysis

Dispersion ability of Fe_3O_4, Fe_3O_4-TiO_2 and FMT as period of time were shown in Fig. 5S. It can be seen, the prepared Fe_3O_4 settled (precipitated) on the bottom of solution and became

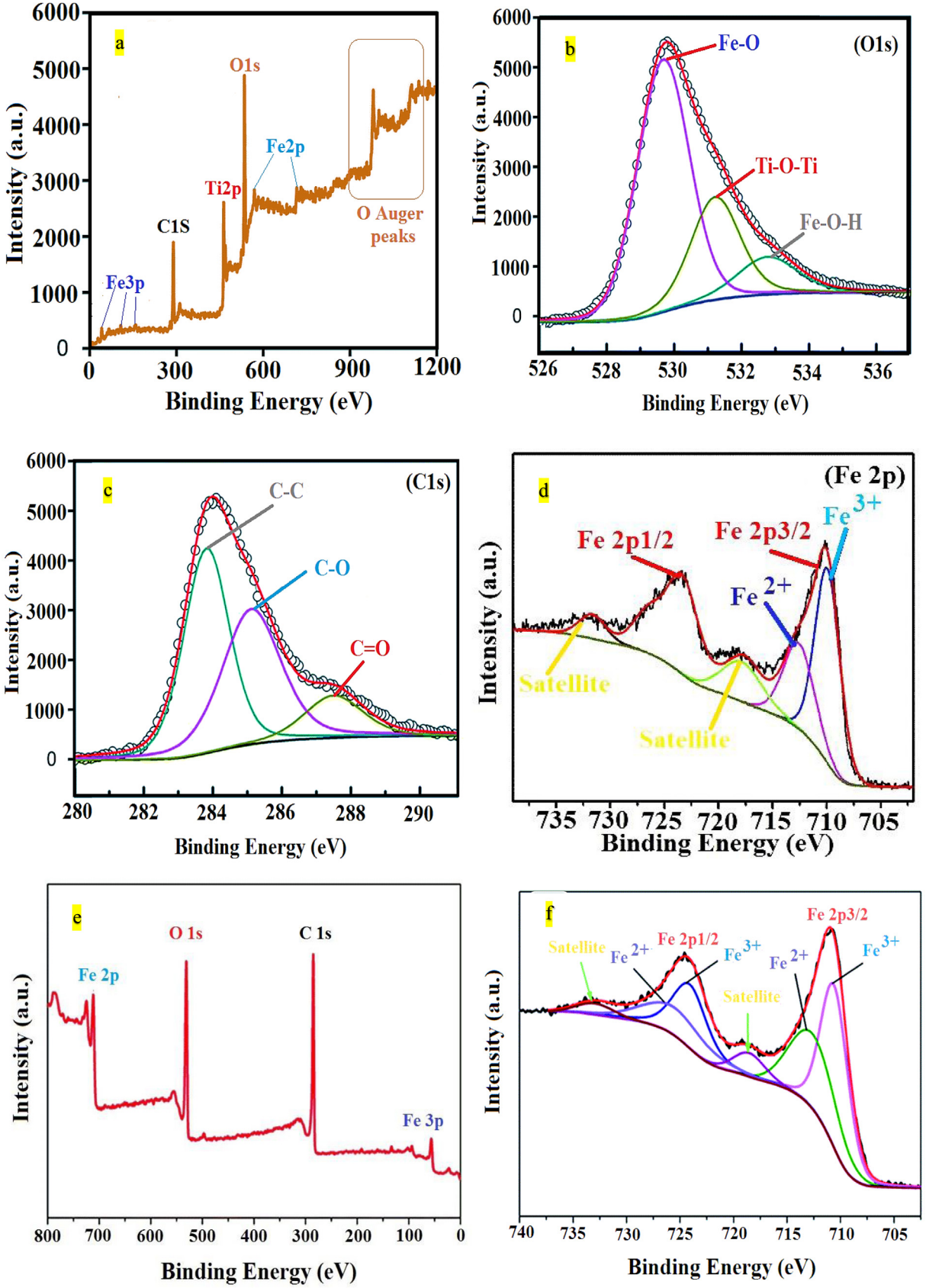

Fig. 3. XPS spectra for FTM: (a) survey, (b) O1s, (c) C1s, and (d) Fe2p. XPS spectra of FTM after degradation: (e) survey, (f) Fe2p.

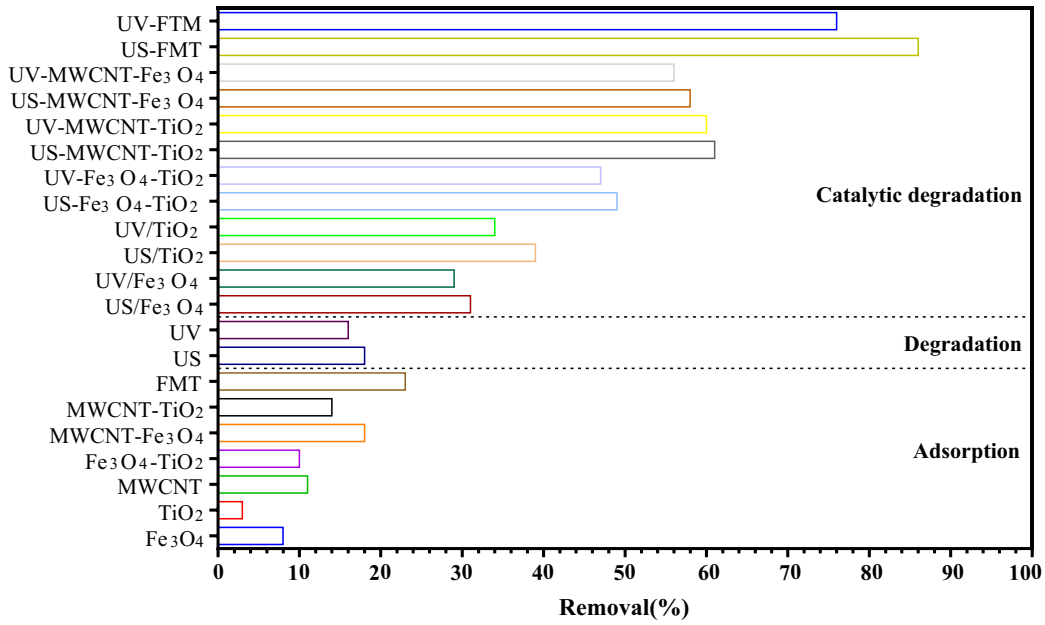

Fig. 4. Comparison the single and composite systems in Sono and photo catalytic removal of 2CP: catalyst dosage 0.2 g L^{-1}, pH 7, Initial concentration 2 mg L^{-1} under 30 min.

aggregation (exposed surface area reduced), which indicate that Fe_3O_4 after 2 h could not have good efficiency in 2CP removal. Almost similar results were obtained after 3 h for Fe_3O_4-TiO_2 prepared. These results show that with grafting reaction of TiO_2, attractive interparticle van der Waals and magnetic forces decreased. For Fe_3O_4-MWCNT-TiO_2, dispersion could retain black and have no visible precipitation in about 7 days. We think it may be related to the small-size and light-weight of MWCNT. These results indicating that MWCNT has effect on the stability of Fe_3O_4-TiO_2 dispersion. Therefore, MWCNT can be used as stabilizer in preparing of FMT.

3.2. Degradation procedure

3.2.1. Removal of 2CP under different systems

The removal efficiency of 2CP was investigated by exposing the pollutants solution to UV–visible irradiation and US radiation in the absence and presence of various catalyst systems. To obtain an accurate degradation data of the composites, pure adsorption experiments were performed under dark conditions (no US or UV irradiation) and the results are shown graphically in Fig. 4. From the figure, the level of 2CP adsorption by FMT is higher than the other samples i.e. Fe_3O_4, MWCNT, Fe_3O_4-TiO_2, MWCNT-Fe_3O_4, MWCNT-TiO_2 and TiO_2, because it has the biggest BET surface area (Table 3S). However, no significant adsorption efficiency under dark and silent conditions was observed. As illustrated in Fig. 4, 2CP removal was less than 18% when direct UV irradiation or ultrasonic radiation was separately employed in the absence of catalysts. In the aqueous solution, 2CP can undergo sono or photo degradation by two possible mechanisms: (i) direct pyrolysis or photolysis described by the following equations:

$$2CP + US \rightarrow \text{intermediates} \rightarrow \text{degradation products} \quad (4)$$

$$2CP + UV \rightarrow \text{intermediates} \rightarrow \text{degradation products} \quad (5)$$

(ii) reactions with free radicals in solution as shown in Eqs. (6)--(22):

$$H_2O + US \rightarrow OH\cdot + H\cdot \quad (6)$$

$$H\cdot + O_2 \rightarrow \cdot HO_2 \quad (7)$$

$$H\cdot + O_2 \rightarrow OH\cdot + O\cdot \quad (8)$$

$$OH\cdot + OH\cdot \rightarrow H_2O_2 \quad (9)$$

$$\cdot HO_2 + \cdot HO_2 \rightarrow H_2O_2 + O \quad (10)$$

$$H_2O_2 + OH\cdot \rightarrow \cdot HO_2 + H_2O \quad (11)$$

$$O_2 + US \rightarrow \cdot + O\cdot \quad (12)$$

$$O\cdot + O_2 \rightarrow O_2 \quad (13)$$

$$2CP + \text{free radicals produced} \rightarrow \text{intermediates} \rightarrow \text{final products} \quad (14)$$

$$H_2O + UV \rightarrow H_2O\cdot \quad (15)$$

$$UV + H_2O\cdot \rightarrow OH\cdot + H\cdot \text{ or } O + 2H \quad (16)$$

$$OH\cdot + OH\cdot \rightarrow H_2O_2 \text{ or } H_2O + O \quad (17)$$

$$H_2O\cdot \rightarrow OH^- + H^+ \quad (18)$$

$$OH^- + OH^+ \rightarrow H_2O_2 + 2e^- \quad (19)$$

$$OH^- \rightarrow OH\cdot + e^- \quad (20)$$

$$O_3 + OH^- + H^+ \rightarrow 2OH\cdot + 4O_2 \quad (21)$$

$$2CP + \text{free radicals produced} \rightarrow \text{intermediates} \rightarrow \text{final products} \quad (22)$$

The combination of UV irradiation or ultrasonic radiation with Fe_3O_4 (US-Fe_3O_4 and UV-Fe_3O_4) did not significantly improve removal of 2CP (<31%). The limited activity in US-Fe_3O_4 and UV-Fe_3O_4 systems is due to the fact that the cavitation phenomenon

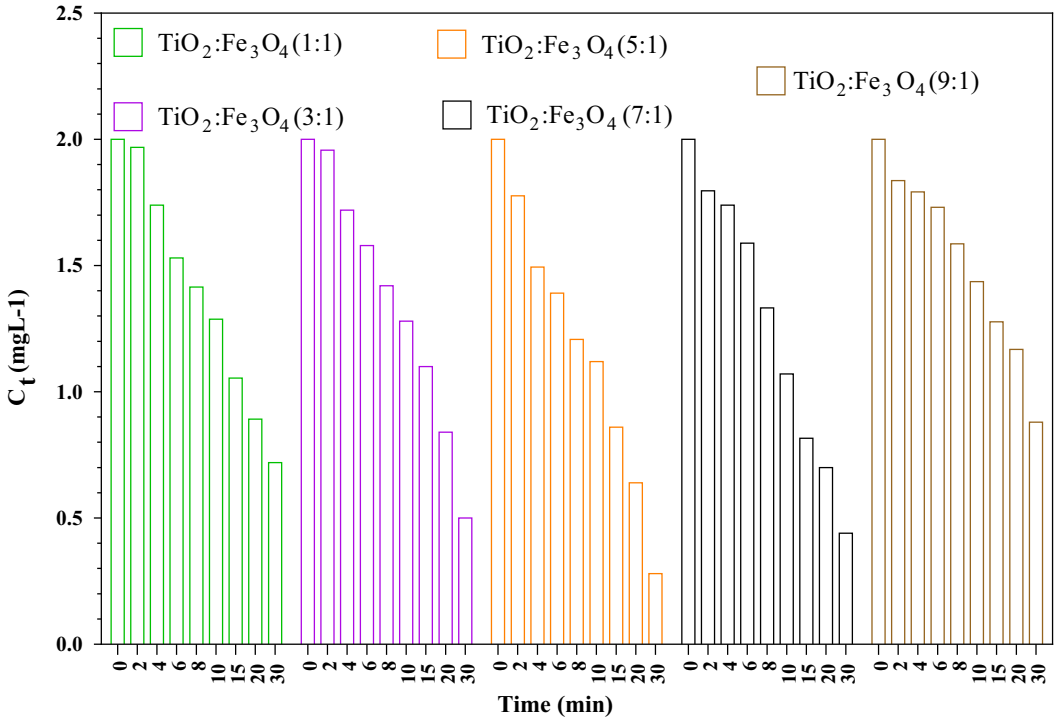

Fig. 5. Degradation of 2CP CP by FMT system at five TiO_2:Fe_3O_4 ratio.i.e. 1:1, 3:1, 5:1, 7:1, 9:1.

ineffectively enhanced the degradation of 2CP in the presence of catalyst [32]. In addition, few active radicals generated during the reaction can be consumed by the iron oxide. The degradation reactions have been summarized as follows:

$$Fe_3O_4 + \text{ US or UV} \rightarrow Fe_3O_4 + h^+ + e^- \quad (23)$$

$$Fe^{3+} + e^- \rightarrow Fe^{2+}, \quad Fe^{2+} + O_2 \rightarrow Fe^{3+} + O\cdot \quad (24)$$

$$h^+ + OH^- \rightarrow H^+ + OH\cdot \quad (25)$$

$$2CP + O\cdot + OH\cdot \rightarrow \text{degradation product} \quad (26)$$

The catalytic degradation of 2CP has been studied by US/TiO_2 and UV/TiO_2 systems. Ultrasonic irradiation of TiO_2 as well as UV irradiation may promote OH· formation on the surfaces of crystals. The effect of TiO_2 may be due to the heterogeneous nucleation of bubbles that enhances the cavitations power. The reactions involved in 2CP degradation under US or UV irradiation has been summarized as follows:

$$TiO_2 + \text{US or UV} \rightarrow h^+ + e^- \quad (27)$$

$$h^+ + H_2O \rightarrow OH\cdot + H^+ \quad (28)$$

$$O_2 + e^- \rightarrow O_2\cdot^- \quad (29)$$

$$O_2\cdot^- + H_2O \rightarrow H_2O_2\cdot^- \quad (30)$$

$$H_2O_2\cdot^- \rightarrow OH^- + OH\cdot \quad (31)$$

$$OH\cdot + O_2\cdot^- + 2CP \rightarrow \text{degradation product} \quad (32)$$

This hybrid catalyst i.e. Fe_3O_4-TiO_2 under both US and UV irradiation has presented greater degradation efficiency instead of using the system individually. The catalytic activity of Fe_3O_4-TiO_2 depends strongly on crystal structure, particle size and surface area. The relatively higher contribution of hybrid catalyst (47–49%) to the 2CP degradation as compared with Fe_3O_4 or TiO_2 can be attributed to the (1) large specific surface area of Fe_3O_4-TiO_2 than Fe_3O_4 or TiO_2 (2) high separation of electron–hole pairs and (3) semiconducting characteristic of Fe_3O_4 shell which can generate highly active electrons and holes under ultrasonic and photocatalytic treatment [33,34]. The hybrid catalyst degradation mechanism:

$$Fe_3O_4 - TiO_2 + \text{ US or UV} \rightarrow Fe_3O_4(h^+.e^-) - TiO_2 \quad (33)$$

$$Fe_3O_4(h^+.e^-) - TiO_2 \rightarrow Fe_3O_4(h^+) - TiO_2(e^-) \quad (34)$$

$$TiO_2\ (e^-) + O_2 \rightarrow O_2\cdot^- + TiO_2 \quad (35)$$

$$Fe_3O_4(h^+) + OH^- \rightarrow OH\cdot \quad (36)$$

$$h^+ + H_2O \rightarrow OH\cdot + h^+ \quad (37)$$

$$h^+ + OH\cdot + O_2\cdot^- + 2CP \rightarrow \text{degradation product} \quad (38)$$

In the MWCNT-TiO_2-US and MWCNT-TiO_2-UV catalytic system, the removal efficiency of 2CP was <61%. In this system, the presence of support (MWCNTs) in FMT structure played an important role in the enhancement of 2CP degradation level as compared to alone TiO_2-US and TiO_2-UV systems [35]. In a FMT catalytic system, the MWCNTs can control the aggregation and improves the solubility and dispersion stability of catalyst in solution which leads to degradation of 2CP was significantly enhanced. The catalytic degradation of 2CP by MWCNT-TiO_2 nanocomposite can be explained by fallowing equations:

$$TiO_2 + \textbf{US} \text{ or } \textbf{UV} \rightarrow h^+ + e^- \quad (39)$$

$$TiO_2(e^-) + MWCNT \rightarrow TiO_2^+ + MWCNT(e^-) \quad (40)$$

$$MWCNT(e^-) + O_2 \rightarrow O_2\cdot^- + MWCNT \quad (41)$$

Table 1
Influence of various parameters on the kinetic of 2CP degradarion.

Parameter	Value	Equation	k_0 (min^{-1})	R^2	$t_{1/2}$(min)
TiO_2:Fe_3O_4 ratios	1:1	y = 0.0363x + 0.0255	0.0363	R^2 = 0.971	19.09091
	3:1	y = 0.0464x − 0.0399	0.0464	R^2 = 0.9949	14.93534
	5:1	y = 0.0627x − 0.0168	0.0627	R^2 = 0.9894	11.05263
	7:1	y = 0.0526x − 0.0038	0.0526	R^2 = 0.982	13.1749
	9:1	y = 0.0272x + 0.0143	0.0272	R^2 = 0.9912	25.47794
Catalyst dosage	0.05	y = 0.0337x + 0.1056	0.0337	R^2 = 0.8713	20.5638
	0.1	y = 0.0769x + 0.0296	0.0769	R^2 = 0.9098	9.011704
	0.2	y = 0.1116x + 0.042	0.1116	R^2 = 0.9695	6.209677
	0.4	y = 0.1917x − 0.2795	0.1917	R^2 = 0.9617	3.615023
	0.6	y = 0.0838x + 0.1603	0.0838	R^2 = 0.9307	8.26969
	0.8	y = 0.0574x + 0.1905	0.0574	R^2 = 0.9018	12.07317
	1	y = 0.0421x + 0.1822	0.0421	R^2 = 0.8805	16.46081
2CP concentration	1	y = 0.2811x − 0.2124	0.2811	R^2 = 0.9331	2.465315
	2	y = 0.1917x − 0.2795	0.1917	R^2 = 0.9617	3.615023
	3	y = 0.085x + 0.0868	0.085	R^2 = 0.9717	8.152941
	4	y = 0.0656x + 0.0262	0.0656	R^2 = 0.9871	10.56402
	5	y = 0.0272x + 0.0824	0.0272	R^2 = 0.9032	25.47794
Initial pH	3	y = 0.2228x − 0.2766	0.2228	R^2 = 0.9704	3.110413
	5	y = 0.3717x − 0.3625	0.3717	R^2 = 0.8544	1.864407
	7	y = 0.1917x − 0.2795	0.1917	R^2 = 0.9617	3.615023
	9	y = 0.0574x + 0.1905	0.0574	R^2 = 0.9018	12.07317
	11	y = 0.0249x + 0.1418	0.0249	R^2 = 0.851	27.83133
Temperature	15	y = 0.052x + 0.0329	0.052	R^2 = 0.9958	13.32692
	25	y = 0.0909x + 0.2067	0.0909	R^2 = 0.9316	7.623762
	35	y = 0.1007x − 0.0124	0.1007	R^2 = 0.9939	6.881827
	45	y = 0.0431x + 0.1434	0.0431	R^2 = 0.8872	16.07889
	55	y = 0.0303x + 0.0629	0.0303	R^2 = 0.9438	22.87129
Ultrasonic power	25	y = 0.0355x + 0.0896	0.0355	R^2 = 0.8863	19.52113
	50	y = 0.0993x − 0.1258	0.0993	R^2 = 0.9893	6.978852
	75	y = 0.1343x − 0.0835	0.1343	R^2 = 0.994	5.160089
	100	y = 0.1918x − 0.273	0.1918	R^2 = 0.9649	3.613139

$$O_2\cdot^- + H^+ \rightarrow OH\cdot \quad (42)$$

$$h^+ + H_2O \rightarrow OH\cdot + H^+ \quad (43)$$

$$h^+ + OH\cdot + O_2\cdot^- + 2CP \rightarrow \text{degradation product} \quad (44)$$

Degradation of 2CP was also not significant by MWCNT- Fe_3O_4-US and MWCNT- Fe_3O_4-UV catalytic system. The catalytic degradation can be proposed as following:

$$Fe_3O_4 + \textbf{US or UV} \rightarrow h^+ + e^- \quad (45)$$

$$Fe_3O_4 + MWCNT \rightarrow Fe_3O_4 + MWCNT(e^-) \quad (46)$$

$$MWCNT(e^-) + O_2 \rightarrow O_2\cdot^- + MWCNT \quad (47)$$

$$Fe_3O_4(h^+) + OH^- \rightarrow OH\cdot + Fe_3O_4 \quad (48)$$

$$h^+ + OH\cdot + O_2\cdot^- + 2CP \rightarrow \text{degradation product} \quad (49)$$

Moreover, in all systems, presence of Fe_3O_4 and hydrogen peroxide (if produced in reactions) can enhance degradation rate by heterogeneous Fenton-like reaction as follow:

$$Fe^{2+} + H_2O_2 \rightarrow Fe^{3+} + OH\cdot + OH^- \quad (50)$$

$$Fe^{3+} + H_2O_2 \rightarrow Fe^{2+} + HOO\cdot + H^+ \quad (51)$$

Fig. 4 also depicts the effect of FMT on the catalytic degradation of 2CP under US and UV irradiation. As shown, the degradation efficiency in FMT-US system dramatically increased to 86% after 30 min while maximizing efficiency in the second system after same time reached to 76%, which implied that ultrasound might play an important role in the activation of catalyst. This phenomenon can be explained by several reasons: (1) the surface area of the catalyst was increased after ultrasonic irradiation, which was in favor of an increase in activity, (2) decrease in the aggregate size of the catalyst, resulting to the more available active sites on the catalyst surface in the FMT system, (3) prevent clustering or agglomeration of magnetic catalysts after the degradation process [36]. All of the above, points out that the increase in the surface area of the catalyst will lead to the improvement of the mass transfer between solute reagents and the solid particles, which subsequently causes a dramatic increase in degradation . [37] Moreover, the clean-up process of the catalyst surface by continuous ultrasonic irradiation may result in the continuous removal of reaction intermediates from the surface, which allowed new reactions occur at the surface [32]. In the following, to better understanding about FMT-US systems, its mechanisms will be discussed. Generally, the results show that the performance of FMT-US systems is higher than that other one, therefore the best process, i.e. FMT-US systems, was selected to future experiments.

3.2.2. Effect of operational parameters on FMT-US systems

3.2.2.1. Effect of TiO_2:Fe_3O_4 ratio. Fig. 5 presents the sonodegradation of 2CP by FMT system at five TiO_2:Fe_3O_4 ratio (1:1, 3:1, 5:1, 7:1, 9:1) under 30 min US irradiation, pH 7 and 0.2 g weight of the catalysts. According to result, 2CP degradation efficiency was the highest when TiO_2 doping ratio was 5:1. The deposited TiO_2 produce e^- and h^+ under US irradiation, which could increase OH· concentration and resulted in improvement of 2CP degradation efficiency. With further increase of TiO_2 ratio to >5:1, TiO2 could occupy the active sites of Fe_3O_4, as a consequence, inhibiting Fenton reaction, H_2O_2 decomposition and formation of hydroxyl radicals on the surface of the catalyst. In addition, the active surface sites of Fe_3O_4 was covered by TiO_2 which was consistent with BET analysis (Table 3S), where the sample with TiO_2:Fe_3O_4 ratio

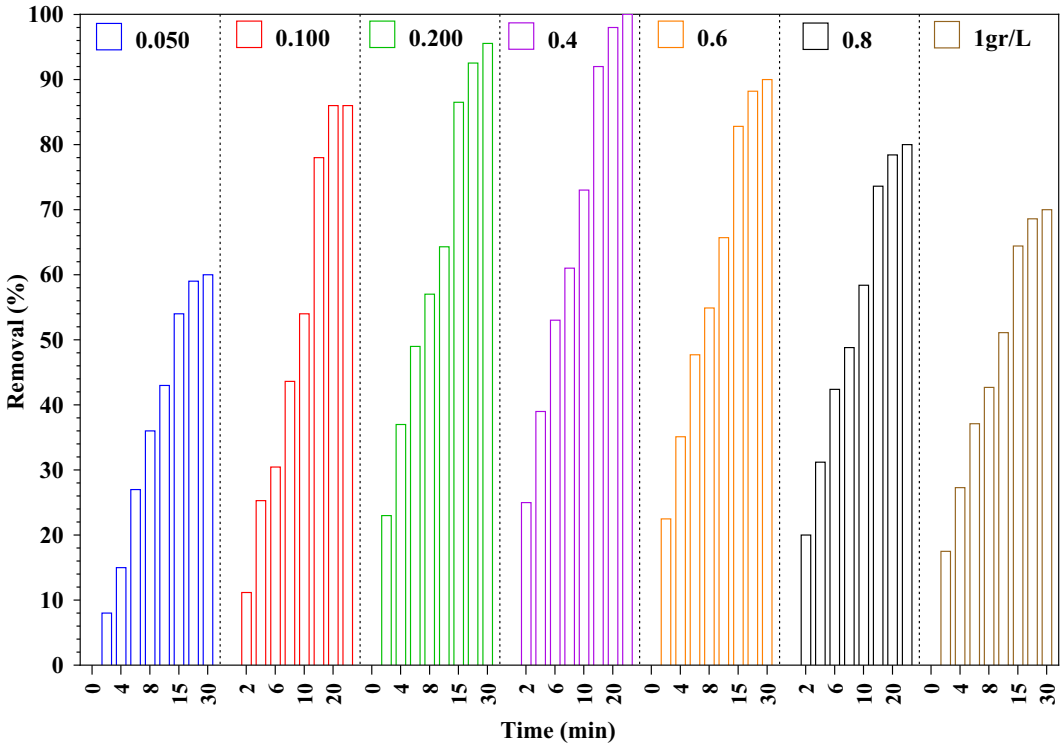

Fig. 6. Effect of the FMT dosage on the sonocatalytic degradation of 2CP.

more than 5:1 had the lowest surface area (active site). In simple terms, the small size of the anatase NPs of the shell by Fe_3O_4 doping, that making the 5:1 TiO_2:Fe_3O_4 possess high-specific surface, thus they can effectively adsorb more molecules and also offer more reaction sites. In addition, by considering the fact that the sonocatalytic activity has a meaningful relationship with band gap energy of the samples, this parameter (Eg) for all TiO_2:Fe_3O_4 ratio were measured by model proposed by Mott and Davis. A Tauc. By plotting $(\alpha h\upsilon)^2$ as a function of photon energy ($h\upsilon$) (Fig. 6S) and extrapolating the linear regions of this curve to $(\alpha h\upsilon)^2 = 0$, the value of Eg. for TiO_2:Fe_3O_4 with ratio equal 5:1 was obtained as 1.75 eV which is lower than the other ratios were examined. In other side, K values (first-order kinetics coefficient (for TiO_2:Fe_3O_4 at 1:5 ratio is more than other systems. (Table 1). Thus, according to the band gap energy and first-order kinetics coefficient, can be stated that FMT with ratio of 5:1 is suitable for exhibiting high sonocatalytic activity compared to other samples. Furthermore, some researchers reported that higher TiO_2 mass ratios with attached to the MWCNTs and covers the entire surface leading to the loss of the MWCNTs role in the composite structure. As previously mentioned the MWCNTs acted as a "dispersing template or support" that controlled the morphology of the TiO_2-Fe_3O_4 nanoparticles in the FMT systems, preventing agglomeration and serving as a reservoir of electrons to trap electrons and prolong the lifetime of the e/h pairs.

3.2.2.2. Effect of catalyst dosage and 2CP concentration. The sonocatalytic degradation of 2CP has been carried out at different initial concentrations ranging from 1 to 5 mg L^{-1} using various FMT dosage from 0.05 g L^{-1} to 1 g L^{-1}, ultrasonic frequency of 50 W and at pH 7. Significant increase in the degradation rate of the 2CP has been observed with an increase in the catalyst dosage (Fig. 6). Results reveal that an optimal dose of 0.4 g of FMT is required for achieving most effective degradation results in the time span of just 15 min; it has been fixed as constant for further studies. Increasing sonocatalyst dosage leads to an increase in the active sites of catalyst which favors the formation of cavities as well as surface cavitation, resulting in improved production of free active radicals which are responsible for sonocatalytic degradation of 2CP. But at the same time, higher catalyst dosage (>0.4 g L^{-1}) also play negative role in degradation process. Increasing the sonocatalyst dosage up to a specific value leads to the aggregation of sonocatalyst particles in the solution, decreasing the number of active sites for the generation of $OH^{\cdot}$ [38]. In other words, the aggregation of sonocatalyst particles deactivates surface active sites of the sonocatalyst responsible for the generation of free oxygen radicals. Moreover, the excess amount of sonocatalyst results in the scattering of ultrasonic irradiation near to the sonocatalyst surface, reducing the rate of sonocatalytic degradation. The excess amount of the sonocatalyst leads to the increased consumption of free radicals at the liquid–gas interface and the increased accumulation of sonocatalytic by-products in the cavitation bubbles, resulting in less powerful collapses for the generation of free radicals [39].

Fig. 7 shows how the variations of the initial 2CP concentration (ranged between 1 and 5 mg L^{-1}) affect its sonocatalysis over FMT nanocomposite while pH, catalyst dosage and power of ultrasonic generator were set to 7, 0.4 gr L^{-1} and 50 W, respectively. It has been found that the removal efficiency is inversely proportional to the initial concentration of 2CP. An explanation to this behavior is that when the initial concentration of 2CP increases, the number of 2CP molecules that adsorbed on the surface of FMT increased, resulting high number of hydroxyl radicals is required for the degradation of pollutant molecules. Nevertheless, the production of hydroxyl radicals remains constant for a given irradiation time, ultrasonic power and catalyst dosage.

3.2.2.3. Effect of pH. pH of the solution with effects on surface charge of the catalyst and pollutant plays a key role in the catalytic degradation of 2CP. Therefore, the effect of pH on the sonocatalytic

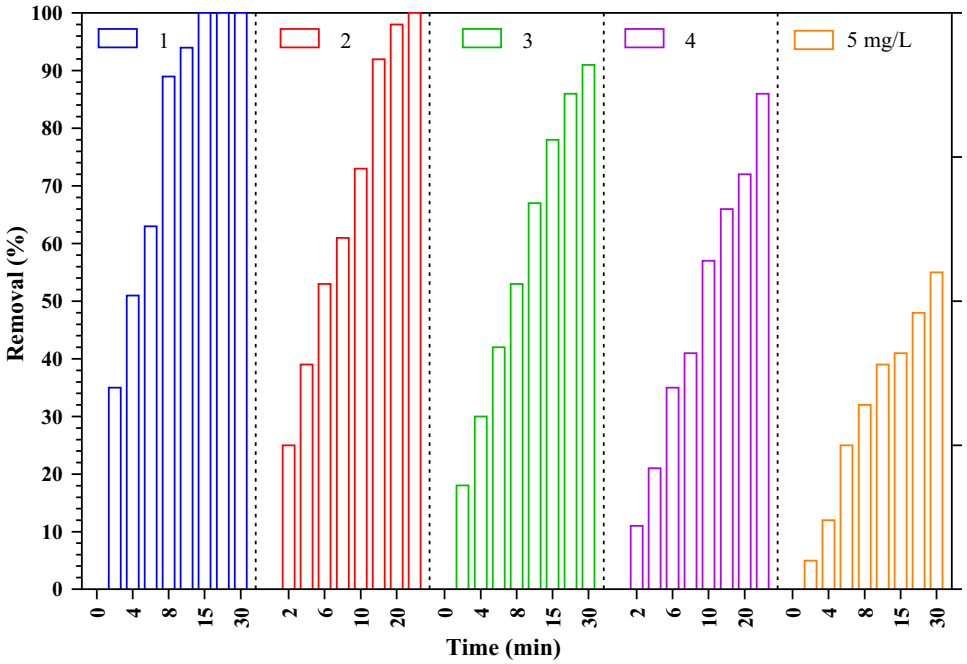

Fig. 7. Effect of the initial concentration of 2CP on the degradation efficiency.

degradation has been investigated within the pH range of 3–11 under FMT-US system. As seen in Fig. 8a, the alkaline pH did not show considerable influence on the concentration of the 2CP, whereas a significant decrease in concentration occurred in the acidic solution (pH 5). 2CP removal efficiencies of 47.84% and 100% were achieved at pH 12.0 and 5.0, respectively. The enhanced oxidation efficiency at lower pH might be due to the following reasons: at lower pH values, the higher dissolution of iron species can accelerate the reaction on the surface of catalyst, and it is benefit to the production of hydroxyl radicals. This is because at acidic pH values, Fe(III) is mainly in the dissolved form and $FeOH^{2+}$ is the most sonoactive Fe (III) species [40]. Upon pH increase, dimeric and oligomeric Fe(III) compounds up to Fe(III) colloids tend to prevail over mononuclear species. The main difference between monomeric and dimeric/oligomeric species or colloids is that the irradiation of the former yields $HO^{\cdot}$ with reasonable to elevated quantum yield, while $HO^{\cdot}$ production by dimeric/oligomeric colloids is quite low. The zeta potential of the FMT (pHpzc = 6.8) may further prove the above explanation to some extent. FMT is positively charged at pH values <pHzpc, whereas it is negatively charged in alkaline solution. Since 2CP is an anionic, electrostatic interactions between the positive FMT surface and 2CP molecules lead to the strong interaction of each other, and it is simple for 2CP molecules to be adsorbed on the FMT surface under the acidic condition. Because the lifetimes of OH radicals are relatively short and they are unlikely to diffuse far from the FMT surface, the degradation process of 2CP seems to occur on the surface of FMT, and not in bulk solution. Thus the electrostatic interactions between the FMT surface and 2CP anion may be responsible for the increase in the degradation ratio in the acidic solution. In contrast, at high pH values (pH > pHpzc), the surface of the catalyst gets negatively charged, which not favors. This is due to the repulsive forces between negative groups of 2CP and negatively charged of FMT (Fig. 8b).

3.2.2.4. Effect of solution temperature and ultrasonic power on degradation efficiency. In order to verify whether the variation of temperature effect on the 2CP degradation, five different temperature value (15–55 °C) were performed to in the FMT-US system. The results showed in the Fig. 9 revealed that the increase of reaction temperature from 15 to 35 °C favored the degradation of 2CP, while further increase in the temperature up to 35 °C led to a decrease in the 2CP removal (60.1%). Increasing the 2CP removal in the first part of solution temperature rising (from 15 to 35 °C) could be ascribed to the higher mass transfer rate, resulting in the enhanced reaction rate of hydroxyl radicals with the considered pollutant [41]. However, in the second part of the temperature increasing, removal efficiency dropped which could be attributed to the degassing of the solution because of the volatilization of gas bubbles, reducing the number of gas nuclei to form cavitation bubbles [42]. In addition, increasing the solution temperature up to a specific value leads to the increase of vapor pressure, leading to the cushion the collapse and consequently, decreasing the generation of OH [23]. In addition, the correlation between the reaction rate and temperature was fitted with the Arrhenius relationship (Figure not shown). The calculated activation energy was to be 19.32 kJ mol^{-1}, revealing the domination of intrinsic chemical reaction in the FMT-US system. Moreover, the lower activation energy demonstrated the more easily activation of FMT in this system. Besides of the solution temperature, Ultrasonic power is another factor that plays an important role in the sonocatalytic degradation process. As shown in the Fig. 9, by increasing the ultrasound power from 25 W L^{-1} to 100 W L^{-1}, the degradation efficiency is increased from 62% to 100%, respectively. Higher degradation efficiency was attained at 100 W ultrasonic power however the operating cost for treating 2CP also have enhanced correspondingly. Thus, given the negligible difference between 100 W and 50 W, this ultrasonic power (50 W) has been chosen for our experimental work. Many reasons can be affected on increasing the efficiency by increasing the ultrasonic power of such as (a) increasing the production of hydroxyl radicals (b) enhance the mass transfer diffusion and (c) improved cavitational instances in the reactor [43]. Of course, this point should not be overlooked that with increasing the ultrasonic power, the energy of cavitation will also increase thereby, enhancing the quality of cavitation bubbles. This will lead to higher reactivity during implosion of cavitation bubbles.

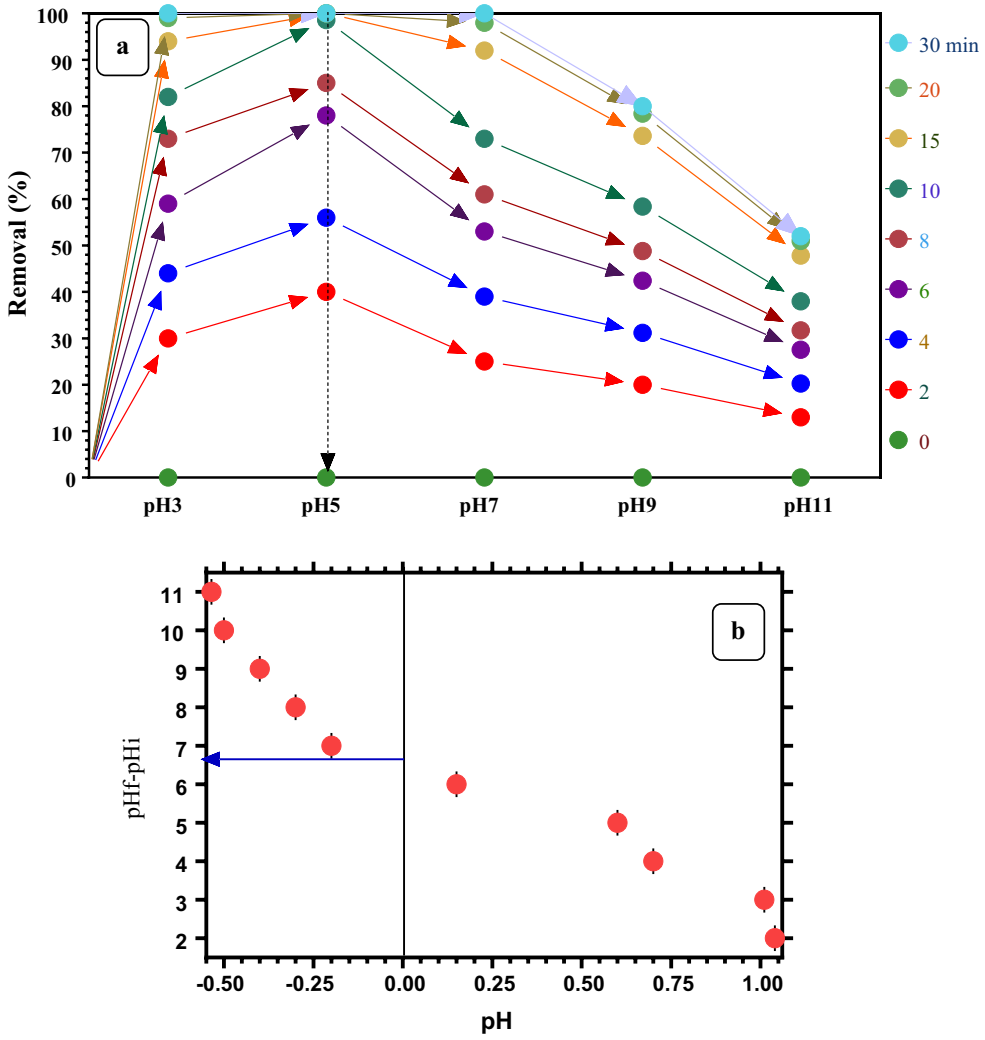

Fig. 8. (a) Influence of pH on 2CP degradation. Reaction conditions: catalyst dose = 0.4 gr L^{-1}, T = 25 C, initial 2CP concentration = 2 mg L^{-1}, ultrasound power = 50 W and (b) zeta potentials of FMT at different pH values.

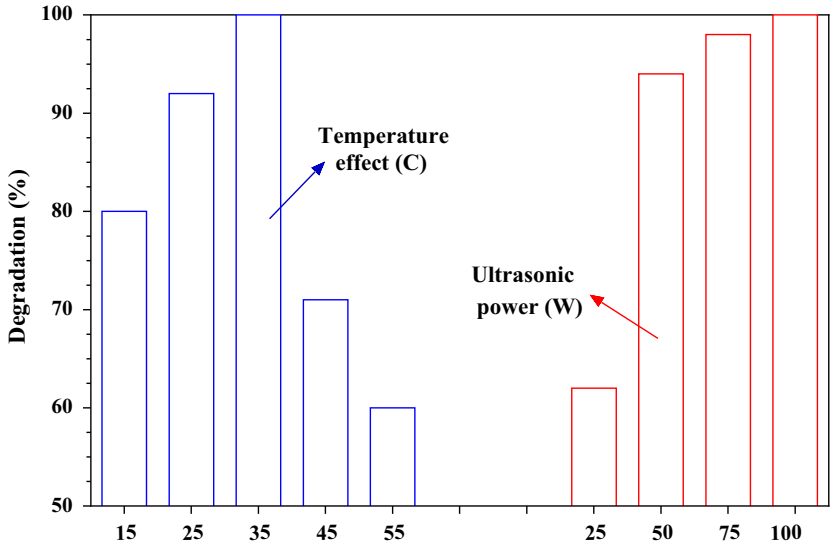

Fig. 9. Effect of (a) solution temperature and (b) ultrasound power on the of 2CP degradation. Reaction conditions: catalyst dose = 0.4 gr L^{-1}, initial 2CP concentration = 2 mg L^{-1}, pH of 5 and the reaction time of 15 min.

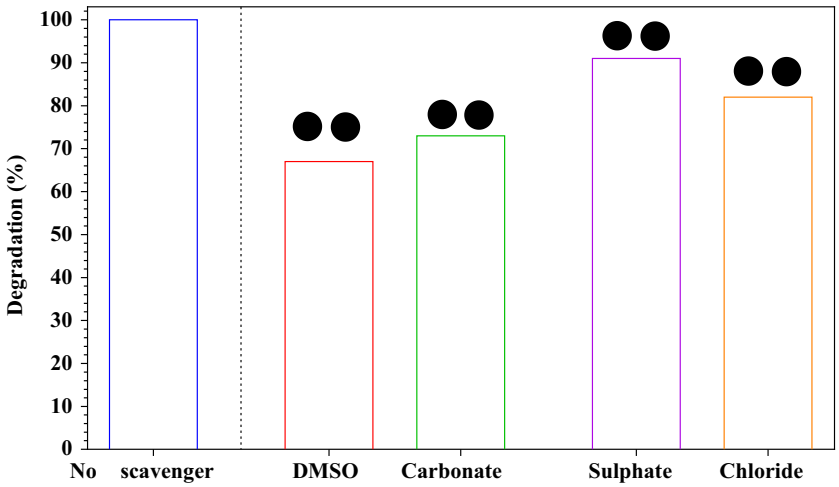

Fig. 10. Sonocatalytic degradation efficiency in the presence of 5 mg $L^{-1}$of different radical scavengers. Reaction conditions: initial 2CP concentration = 2 mg L^{-1} and FMT dosage = 0.4 g L^{-1}. The data are from five experiments with each assay performed in triplicate. Black solid circles: significant difference from control value (No scavenger) ($p < .01$, one-way ANOVA).

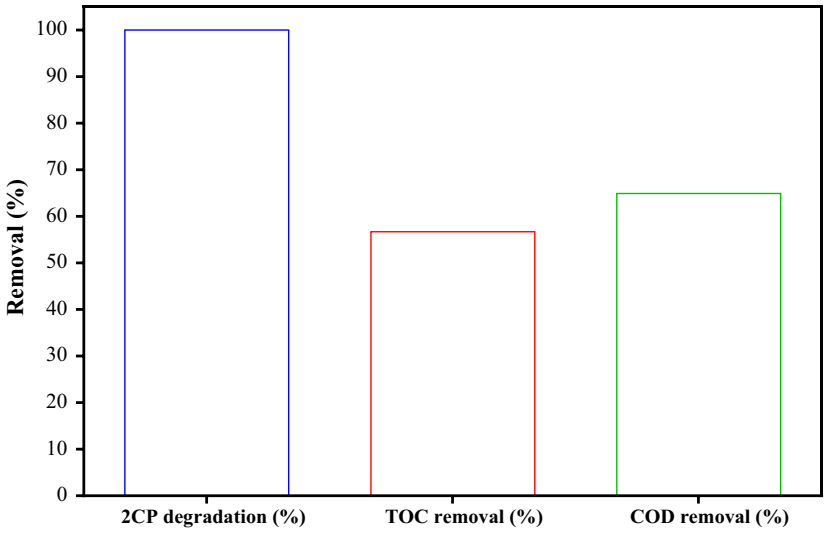

Fig. 11. The change of 2CP, COD and TOC removal (%). Reaction conditions: initial 2CP concentration = 2 mg L^{-1} and FMT dosage = 0.4 g L^{-1} within 15 min.

3.2.3. Influence of hydroxyl radical scavengers

Real wastewater usually contains organic and inorganic species, which can affect the activity of catalysts. To investigate the effect of the ion species on the sonocatalytic degradation process, the studies have been carried out in the presence of dimethyl sulfoxide (DMSO), carbonate, sulphate and chloride, which have hydroxyl radical scavenging property. In this set of experiments, the initial concentration of 2CP, the catalyst dosage, ultrasonic power, the concentration of ionic species was constant at 2 mg L^{-1}, 0.4 g L^{-1}, 50 W and 5 mg L^{-1}, respectively. Experimental results illustrated, degradation efficiency of 2CP decreased in the presence of all used radical scavengers. According to the obtained results, the degradation efficiency decreased from 100% to 67%, 82%, 73% and 91%, in the presence of DMSO, chloride, carbonate and sulfate ions, respectively at the reaction time of 10 min (Fig. 10). Statistical analysis (one-way ANOVA) indicated that the difference in degradation ratio between the control group (no scavenger) and the radical scavenger-containing groups (i.e., DMSO, chloride, carbonate and sulfate ions) were significant ($P < .01$). Among the scavengers, DMSO was the most effective ($n = 5$). The results confirmed that the free radical attack mechanism play an important role in the FMT-US-induced degradation of 2CP. The possible reactions that can occur in the presence of the radical scavengers are as follows:

$$Cl^- + h^+ \rightarrow Cl\cdot \quad (52)$$

$$Cl\cdot + Cl^- \rightarrow Cl_2\cdot^- \quad (53)$$

$$Cl^- + OH\cdot \rightarrow Cl\cdot + OH^- \quad (54)$$

$$SO_4^{2-} + OH\cdot \rightarrow SO_4\cdot^- + OH^- \quad (55)$$

$$CO_3^{2-} + OH\cdot \rightarrow \cdot^- + OH^- \quad (56)$$

$$(CH_3)_2SO + OH\cdot \rightarrow CH_3\,SO_2H + CO_3\cdot \quad (57)$$

3.2.4. Mineralization assessment and mean intermediates

TOC and COD were measured to investigate the mineralization efficiency of 2CP in the FMT-US system. This set of experiments

was performed at optimized conditions i.e. the initial 2CP concentration of 2 mg L^{-1}, the sonocatalyst dosage of 0.4 g L^{-1} and the initial pH of 5. From Fig. 11, at the same operational conditions 100% of 2CP removal obtained within 15 min, while over same minutes of process, removal efficiencies of TOC and COD were 56.7% and 64.9%, respectively. In fact, some 2CP molecules could be degraded into H_2O and CO_2 during the sonocatalysis process, whereas other sections of 2CP molecules were decomposed into the intermediate byproducts. These organic byproducts (chlorinated aromatic rings) are difficult to further degrade than 2CP molecules; thus, the removal of TOC and COD were much less than the degradation efficiency (%) of 2CP under the same experimental conditions. According to important role of intermediates on removal of TOC and COD, GC-MS was used to identify intermediates of 2CP degradation in FMT-US system. Hydroquinone ($C_6H_6O_2$), benzoquinone ($C_6H_4O_2$), and a mixture of carboxylic acid substrates i.e. maleic acid ($C_4H_4O_4$), fumaric acid ($C_4H_4O_4$), oxalic acid ($C_2H_2O_4$), and formic acid (CH_2O_2), were the main intermediate compounds identified during 2CP degradation process. Fig. 7S shows the suggested pathway of 2CP oxidation: first, the Chlorine (Cl) atom removes from 2CP, after which Superoxide ($O2^{\cdot}-$) and hydroxyl ($OH^{\cdot}$) radicals attack the compound to generate $C_6H_6O_2$. Hydroquinone molecules are subsequently dehydrogenated to $C_6H_4O_2$. The availability of excess free radicals breaks the benzoquinone ring to produce aliphatic carboxylic acids, including $C_4H_4O_4$ and $C_4H_4O_4$. Further oxidation of maleic acid produces $C_2H_2O_4$, the subsequent oxidization of which produces formic CH_2O_2, finally, carbon dioxide.

3.2.5. Rate kinetic modelling

The sonocatalytic degradation mechanism and kinetics of 2CP were studied using Langmuir– Hinshelwood (L–H) model. Following equation expressed the L–H kinetic model [44,45]:

$$\mathbf{r} = -\frac{\mathbf{dc}}{\mathbf{dt}}\mathbf{k_r}\theta = \frac{\mathbf{k_r KC}}{1+\mathbf{KC}} \tag{63}$$

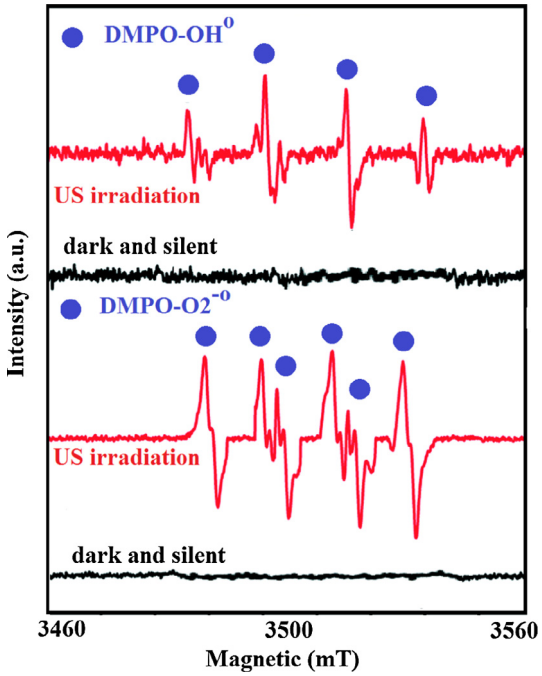

Fig. 12. EPR spectra in US-FMT system. Reaction conditions: catalyst dose = 0.4 g L^{-1}, T = 35 C, 2CP concentration = 2 mg L^{-1}, ultrasound power = 50 W, [DMPO] = 0.1 M.

where r is the reaction rate, k_r is the reaction rate constant, K is the reactant adsorption constant, h is the fraction of the surface of catalyst covered by 2CP, and C is the concentration of 4-CP at any time t. Eq. (63) can be simplified to a first order reaction when C is very low, in which case one has:

$$\mathbf{r} = -\frac{\mathbf{dc}}{\mathbf{dt}}\mathbf{k_r KC} = \mathbf{k_0 t} \tag{64}$$

where $\mathbf{k_0} = \mathbf{k_r K}$

The integration of Eq. (64) gives:

$$\ln\frac{\mathbf{C_0}}{\mathbf{C_t}} = \mathbf{k_0 t} \tag{65}$$

where $\mathbf{C_0}$ is the initial concentration of 2CP, $\mathbf{C_t}$ is the concentration of 2CP at time $\mathbf{t}$, $\mathbf{k_0}$ is the first-order reaction rate constant (min^{-1}), and t is the reaction time (min). By plotting $\ln(\mathbf{C_0}/\mathbf{C})$ versus t, the apparent rate constant ($\mathbf{k}$) can be determined from the slope of the curve obtained. The time required for concentration of the reactant to drop to half its value is called the reaction's half-time or half-life ($\mathbf{t_{\frac{1}{2}}}$). Half-life for first-order reaction could also be calculated by:

$$\mathbf{t}_{\frac{1}{2}=\frac{0693}{\mathbf{k}}} \tag{57}$$

In present study, the influence of studied parameters including Fe_3O_4-TiO_2 ratios, Catalyst dosage, initial 2CP concentration, initial pH, temperature and ultrasonic power on the kinetic of 2CP degradation was investigated. The values of first-order reaction rate constant k related to the various parameters along with their regression coefficients R^2 are given in Table 1. In all the experiments, the high regression coefficient (>0.8544) supported the fitting of sonocatalytic degradation of 2CP by first-order reaction kinetic model. From Table 1, it can observe that the rate constants strongly depend on Initial pH. For example, at initial pH 5, the degradation rate of 2CP increased to 0.3717 min^{-1}, while the amount of k_0 in pH 11 was equal 0.0574 min^{-1}

3.2.6. Mechanism of ultrasonic degradation

To characterize the formation of the generated radical species over FMT under simulated ultrasound irradiation, ESR techniques coupled with DMPO were employed. The typical four peaks (Fig. 12) in the spectra with intensity ratio of 1:2:2:1 could be assigned to DMPO-$OH^{\cdot}$, indicating OH radical generated at the initial phase under irradiation. No ESR signal is observed for these samples in the dark and silent conditions. On the other hands, electrons in the conduction band can be rapidly trapped by molecular oxygen adsorbed on the catalyst particle, which is reduced to form superoxide radical anion [46] (E $O_2/O_2^{-\cdot}$ = −0.16 V). Therefore, the formation of superoxide radicals was also examined by DMPO spin trapping ESR techniques in methanolic media. As shown in Fig. 12, six characteristic peaks of the DMPO-$O_2^{-\cdot}$ adducts were observed on FMT system under ultrasonic irradiation. By contrast, there are no signals detected in blank test. These results elucidated that superoxide radicals were efficiently generated under FMT-US system. Based on the results, a possible sonocatalytic process for the degradation of 2CP under ultrasonic irradiation are proposed: Upon ultrasonic irradiation, TiO_2 undergo charge separation to yield electrons (e^-) and holes (h^+). Since the MWCNTs are known as good electron acceptors, the electrons on conduction band of the TiO_2 rapidly transfer to MWCNTs. The negatively charged MWCNTs (e^-) can react with the O_2 to produce the active species $O_2^{-\cdot}$ radicals which reacts with hydrogen ions (H^+) to produce hydroxyl radicals ($OH^{\cdot}$), which oxidizes the adsorbed 2CP directly on the surface. At the same time, the holes from TiO_2 react with adsorbed water to further produce hydroxyl radicals. Finally, the active species (h^+, $O_2^{-\cdot}$ and $OH^{\cdot}$ radicals) oxidize the 2CP molecules adsorbed on these active sites of the FMT system through π-π stacking interactions

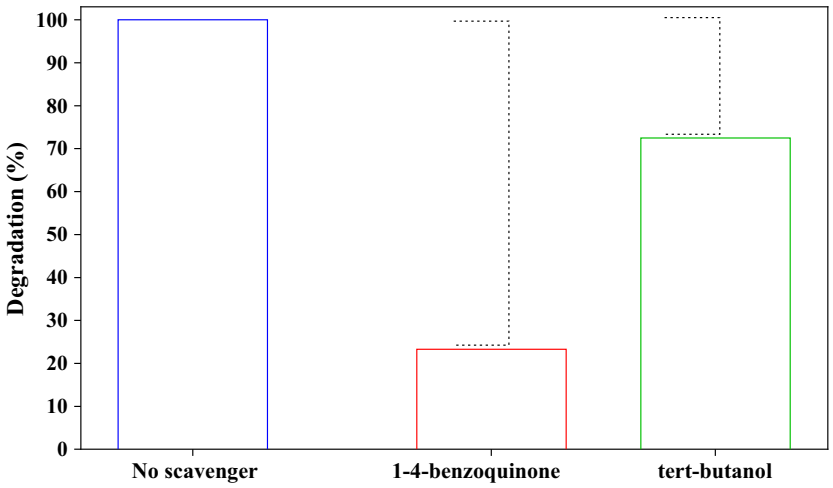

Fig. 13. Inhibition effect of 1,4-benzoquinone and tert-butanol on 2CP degradation using US-FMT system. Reaction conditions: catalyst dose = 0.4 g L^{-1}, T = 35 C, 2CP concentration = 2 mg L^{-1}, ultrasound power = 50 W.

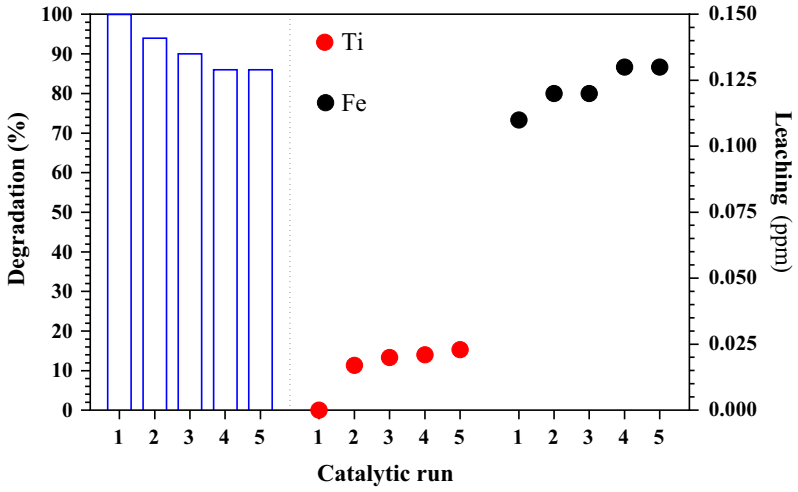

Fig. 14. Reusability and leaching of the FMT sonocatalyst during 5 consecutive runs. Reaction conditions: catalyst dose = 0.4 g L^{-1}, T = 35 C, 2CP concentration = 2 mg L^{-1}, ultrasound power = 50 W.

and/or electrostatic interaction. Based on the above analysis, the degradation mechanisms is proposed as follows (Schematic S1):

$$TiO_2 + \mathbf{US} \rightarrow TiO_2(h^+ + e^-) \quad (58)$$

$$TiO_2(e^-) + MWCNTs \rightarrow TiO_2 + MWCNTs(e^-) \quad (59)$$

$$MWCNTs(e^-) + O_2 \rightarrow O_2{\cdot}^- + MWCNTs \quad (60)$$

$$O_2{\cdot}^- + H^+ \rightarrow OH\cdot \quad (61)$$

$$h^+ + H_2O \rightarrow OH\cdot + H^+ \quad (62)$$

$$OH\cdot + O_2{\cdot}^- + 2CP \rightarrow \text{degradation product} \quad (63)$$

During the FMT activation process, Superoxide ($O2^{\cdot -}$) and hydroxyl radical (.OH) were the main radicals generated. In order to identify the dominating radicals for 2CP degradation in the US/FMT system, scavenging experiment was carried out. 1,4-benzoquinone and tert-butanol (TBA) were used as radical scavengers (quenching agents) to identify the oxidizing radical species in a FMT-US system [47]. The results of scavenging experiment were showed in Fig. 13. It can be seen that the addition of both 1,4-benzoquinone and tert-butanol lead to decrease the degradation of 2CPin comparison with the no addition of quenching agent reaction system. These results suggested that radical oxidation ($O2^{\cdot -}$ and $OH^{\cdot}$) is the dominant mechanism in degradation of 2CP by FMT-US system. As depicted in Fig. 13, by adding TBA, oxidation efficiency reached to 72.5%. However, since 2CP degradation efficiency decreased to 23.3% in the present of 1,4-benzoquinone, $O2^{\cdot -}$ is considered as the dominant radical species in the FMT-US system.

3.2.7. Reusability of the sonocatalyst

As well as the excellent sonocatalytic activity, the reusability of sonocatalysts are also important parameter in practical applications and its economical point of view. To evaluate the reusability efficiency of the FMT sample, the particle size distribution and magnetic performance of MST were determined under optimized operational conditions. As a result, FMT prior to sonocatalytic test had a size distribution in the ranges 20–50 nm. After sonocatalysis process, FMT was separated and dried prior to particle size distribution analysis. It revealed a size distribution ranging from 39 ± 2 nm (Figure not shown). The homogeneity in the size

distribution might be due to the physical effect of US irradiation [48]. Moreover, magnetic property of FMT after degradation process (Ms = 41.5 emu/g) revealed, sonocatalysts were completely separated by a permanent external magnet. To examine the reusability of the FMT nanocomposite, the sonocatalytic degradation experiments were performed with catalyst dosage of 0.4 g L^{-1}, initial 2CP concentration of 2 mg L^{-1} and the reaction time of 15 min at 35 °C temperature. In each run, the sonocatalytic activity of the recycled FMT nanocomposite exanimated by collecting the nanocomposite from sample solution. The recovered nanocomposite (thoroughly washing with water and ethanol and drying) have developed again to degrade the 2CP repeatedly under ultrasonic irradiation. The results are presented in Fig. 14. As can be seen, the sonodegradation efficiency has negligible drops from 100 to 94%, 90%, 86%, and 85.96%, respectively during five repeated runs. These evidence indicates that the FMT nanocomposite are durable and effective for the remediation of 2CP up to five runs. The partial deactivation of the catalyst is related to some surface poisoning that may be induced by adsorbed intermediates.

3.2.8. Leaching experiment and toxicity evolution

The leaching of Fe and Ti from the FMT system to the solution was determined during five repeated runs and the mass of leached was shown in Fig. 14. It was found that, about 0.130 and 0.025 mg L^{-1} of Fe and TiO_2 leached from the catalyst at 5th runs under optimized condition, respectively. Reutilization tests using FMT revealed some loss in activity (Fig. 14) from the first to the third run, while it was maintained constant after the third run. Similarly, a significant decrease in the amount of leached of Fe and TiO_2 was observed in the 3rd run and almost stabilized after that. This suggests that after some initial Fe and Ti lost by leaching, the catalyst tend to stabilize under continuous use with a significant sonoactivity. However, it should be noted that the amount of leached iron in US-FMT systems did not exceed the legislated limit that can be found in waste waters. As previously stated, even though 100% of 2CP was degraded by FMT-US system, however conversion of 2CP was about 55–65%. In this case, the variation of acute toxicity of product was evaluated by a 48 h immobilization assay with D. magna. A mortality rate of 60% of D. magna was observed in a raw 2CP solution. After 5 min reaction, the toxicity reached a maximum value, and 100% of D. magna was immobilized. The results are probably due to the fact that the by-products of 2CP exhibited higher acute toxicity [48–62], and thereby acute toxicity increased during the first 5 min. When the reaction time was extended to >5 min, the by-products decomposed gradually, leading to the decreased toxicity (55%). Therefore, mare than 5 min reaction time is necessary to reduce acute toxicity for the 2CP treatment.

4. Conclusions

FMT with average size of lower than 60 nm were synthesized and used as reusable sonocatalyst for sonocatalytic removal of 2CP. The removal efficiency of US-FMT was higher than that of other removal systems, and TiO_2:Fe_3O_4 with 5:1 ratio showed the best sonocatalytic performance with a 2CP degradation efficiency of 86%. The effect of different operational parameters including the pH, catalyst dosage, initial 2CP concentration, temperature and ultrasound power was investigated on the sonocatalysis efficiency. The sonocatalytic activity of FMT was attributed to the generation of more hydroxyl and superoxide radicals produced. The synthesized sonocatalyst showed good durability because there was no loss in the removal efficiency of 2CP by sonocatalysis in five repetitive experiments. The intermediates of 2CP degradation were identified by GC-Mass analysis. Given the promising results of this study, more research should be carried out on the use of FMT for the degradation of other organic pollutants in water and wastewater.

Acknowledgment

This work was supported by Bushehr University of Medical Sciences, Bushehr, Iran, (Project No. 4324). A special thanks is also extended to Dr. Ehsan Ahmadi for his cooperation.

Appendix A. Supplementary material

Supplementary data associated with this article can be found, in the online version, at https://doi.org/10.1016/j.jcis.2017.10.015.

References

[1] A.M. Abeish, M. Ang, H. Znad, Enhanced solar-photocatalytic degradation of combined chlorophenols using ferric ions and hydrogen peroxide, Ind. Eng. Chem. Res. 53 (26) (2014) 10583–10589.
[2] J. Lopez, V. Monsalvo, D. Puyol, A. Mohedano, J. Rodriguez, Low-temperature anaerobic treatment of low-strength pentachlorophenol-bearing wastewater, Biores. Technol. 140 (2013) 349–356.
[3] J.A. Field, R. Sierra, Review of scientific literature on microbial dechlorination and chlorination of key chlorinated compounds, Department of Chemical & Environmental Engineering University of Arizona, 2001 37p.
[4] B.A. Lyon, R.M. Cory, H.S. Weinberg, Changes in dissolved organic matter fluorescence and disinfection byproduct formation from UV and subsequent chlorination/chloramination, J. Hazard. Mater. 264 (2014) 411–419.
[5] A.O. Olaniran, E.O. Igbinosa, Chlorophenols and other related derivatives of environmental concern: properties, distribution and microbial degradation processes, Chemosphere 83 (10) (2011) 1297–1306.
[6] F. Maqbool, S. Mostafalou, H. Bahadar, M. Abdollahi, Review of endocrine disorders associated with environmental toxicants and possible involved mechanisms, Life Sci. 145 (2016) 265–273.
[7] M.V. Bagal, P.R. Gogate, Wastewater treatment using hybrid treatment schemes based on cavitation and Fenton chemistry: a review, Ultrason. Sonochem. 21 (1) (2014) 1–14.
[8] M.F.A. Taleb, Adsorption and photocatalytic degradation of 2-CP in wastewater onto CS/$CoFe_2$ O_4 nanocomposite synthesized using gamma radiation, Carbohydr. Polym. 114 (2014) 65–72.
[9] M.A. Ajeel, M.K. Aroua, W.M.A.W. Daud, Anodic degradation of 2-chlorophenol by carbon black diamond and activated carbon composite electrodes, Electrochim. Acta 180 (2015) 22–28.
[10] R. Jusoh, A. Jalil, S. Triwahyono, A. Idris, M. Noordin, Photodegradation of 2-chlorophenol over colloidal α-FeOOH supported mesostructured silica nanoparticles: Influence of a pore expander and reaction optimization, Sep. Purif. Technol. 149 (2015) 55–64.
[11] N. Sharotri, D. Sud, Ultrasound-assisted synthesis and characterization of visible light responsive nitrogen-doped TiO_2 nanomaterials for removal of 2-Chlorophenol, Desalination Water Treat. 57 (19) (2016) 8776–8788.
[12] M. Răileanu, M. Crişan, I. Niţoi, A. Ianculescu, P. Oancea, D. Crişan, L. Todan, TiO2-based nanomaterials with photocatalytic properties for the advanced degradation of xenobiotic compounds from water. A literature survey, Water, Air, Soil Pollut. 224 (6) (2013) 1548.
[13] M. Shahid, A. McDonagh, J.H. Kim, H.K. Shon, Magnetised titanium dioxide (TiO2) for water purification: preparation, characterisation and application, Desalination Water Treat. 54 (4–5) (2015) 979–1002.
[14] Z.-J. Li, Z.-W. Huang, W.-L. Guo, L. Wang, L.-R. Zheng, Z.-F. Chai, W.-Q. Shi, Enhanced photocatalytic removal of uranium (VI) from aqueous solution by magnetic TiO_2/Fe_3O_4 and its graphene composite, Environ. Sci. Technol. 51 (10) (2017) 5666–5674.
[15] M. Lirong, S. Jianjun, Z. Ming, H. Jie, Synthesis of magnetic sonophotocatalyst and its enhanced biodegradability of organophosphate pesticide, Bull. Korean Chem. Soc. 35 (12) (2014) 3521–3526.
[16] M. Qiao, X. Lei, Y. Ma, L. Tian, K. Su, Q. Zhang, Well-defined core-shell Fe_3O_4@ polypyrrole composite microspheres with tunable shell thickness: synthesis and their superior microwave absorption performance in the Ku Band, Ind. Eng. Chem. Res. 55 (22) (2016) 6263–6275.
[17] L. Zhu, Z.-D. Meng, C.-Y. Park, T. Ghosh, W.-C. Oh, Characterization and relative sonocatalytic efficiencies of a new MWCNT and CdS modified TiO_2 catalysts and their application in the sonocatalytic degradation of rhodamine B, Ultrason. Sonochem. 20 (1) (2013) 478–484.
[18] Z. Chen, P. Sun, B. Fan, Z. Zhang, X. Fang, In situ template-free ion-exchange process to prepare visible-light-active g-C3N4/NiS hybrid photocatalysts with enhanced hydrogen evolution activity, J. Phys. Chem. C 118 (15) (2014) 7801–7807.
[19] A. Makama, A. Salmiaton, E. Saion, T. Choong, N. Abdullah, Microwave-assisted synthesis of porous ZnO/SnS_2 heterojunction and its enhanced photoactivity for water purification, J. Nanomater. 2015 (2015) 1.

[20] S. Indrawirawan, Graphene-based nanocarbons for catalytic degradation of aqueous contaminants, Curtin University, 2016.
[21] J. Busch, Investigations on mobility of carbon colloid supported nanoscale zero-valent iron (nZVI) for groundwater remediation, 2015.
[22] E. Alves Nunes Simonetti, L.D.S. Cividanes, T.M. Bastos Campos, F. Williams Fernandes, J.P.B. Machado, G.P. Thim, Sonocatalytic degradation of methylene blue in the presence of TiO2 doped carbon nanostructures—catalytic and adsorption comparison by different carbon forms, Fullerenes, Nanotubes and Carbon Nanostructures 23(8) (2015) 725–733.
[23] M. Zhou, H. Yang, T. Xian, R. Li, H. Zhang, X. Wang, Sonocatalytic degradation of RhB over $LuFeO_3$ particles under ultrasonic irradiation, J. Hazard. Mater. 289 (2015) 149–157.
[24] E.A. Serna-Galvis, J. Silva-Agredo, A.L. Giraldo-Aguirre, O.A. Flórez-Acosta, R.A. Torres-Palma, High frequency ultrasound as a selective advanced oxidation process to remove penicillinic antibiotics and eliminate its antimicrobial activity from water, Ultrason. Sonochem. 31 (2016) 276–283.
[25] N. Yuan, G. Zhang, S. Guo, Z. Wan, Enhanced ultrasound-assisted degradation of methyl orange and metronidazole by rectorite-supported nanoscale zero-valent iron, Ultrason. Sonochem. 28 (2016) 62–68.
[26] J.C. Colmenares, W. Ouyang, M. Ojeda, E. Kuna, O. Chernyayeva, D. Lisovytskiy, S. De, R. Luque, A.M. Balu, Mild ultrasound-assisted synthesis of TiO_2 supported on magnetic nanocomposites for selective photo-oxidation of benzyl alcohol, Appl. Catal. B 183 (2016) 107–112.
[27] Z. Zhu, X. Tang, S. Kang, P. Huo, M. Song, W. Shi, Z. Lu, Y. Yan, Constructing of the magnetic photocatalytic nanoreactor MS@ FCN for cascade catalytic degrading of tetracycline, J. Phys. Chem. C 120 (48) (2016) 27250–27258.
[28] A. Taufik, R. Saleh, Synthesis of iron (II, III) oxide/zinc oxide/copper (II) oxide (Fe_3 O_4/ZnO/CuO) nanocomposites and their photosonocatalytic property for organic dye removal, J. Colloid Interface Sci. 491 (2017) 27–36.
[29] B. Liu, W. Zhang, F. Yang, H. Feng, X. Yang, Facile method for synthesis of Fe_3O_4@ polymer microspheres and their application as magnetic support for loading metal nanoparticles, J. Phys. Chem. C 115 (32) (2011) 15875–15884.
[30] S. Guo, G. Zhang, J. Wang, Photo-Fenton degradation of rhodamine B using Fe_2 O_3–Kaolin as heterogeneous catalyst: characterization, process optimization and mechanism, J. Colloid Interface Sci. 433 (2014) 1–8.
[31] X.S. Nguyen, G. Zhang, X. Yang, Mesocrystalline Zn-Doped Fe_3O_4 hollow submicrospheres: formation mechanism and enhanced photo-fenton catalytic performance, ACS Appl. Mater. Interfaces 9 (10) (2017) 8900–8909.
[32] L. Hou, L. Wang, S. Royer, H. Zhang, Ultrasound-assisted heterogeneous Fenton-like degradation of tetracycline over a magnetite catalyst, J. Hazard. Mater. 302 (2016) 458–467.
[33] S. Kumar, B. Kumar, A. Baruah, V. Shanker, Synthesis of magnetically separable and recyclable g-C_3N_4–Fe_3O_4 hybrid nanocomposites with enhanced photocatalytic performance under visible-light irradiation, J. Phys. Chem. C 117 (49) (2013) 26135–26143.
[34] S. Salamat, H. Younesi, N. Bahramifar, Synthesis of magnetic core–shell Fe_3O_4@ TiO_2 nanoparticles from electric arc furnace dust for photocatalytic degradation of steel mill wastewater, RSC Adv. 7 (31) (2017) 19391–19405.
[35] Y.-J. Xu, Y. Zhuang, X. Fu, New insight for enhanced photocatalytic activity of TiO_2 by doping carbon nanotubes: a case study on degradation of benzene and methyl orange, J. Phys. Chem. C 114 (6) (2010) 2669–2676.
[36] T. Chave, N.M. Navarro, P. Pochon, N. Perkas, A. Gedanken, S.I. Nikitenko, Sonocatalytic degradation of oxalic acid in the presence of oxygen and Pt/TiO_2, Catal. Today 241 (2015) 55–62.
[37] N.H. Ince, A. Ziylan, Single and hybrid applications of ultrasound for decolorization and degradation of textile dye residuals in water, Green Chem. Dyes Removal Wastewater: Res. Trends Applications (2015) 261–293.
[38] J. Esmaili-Hafshejani, A. Nezamzadeh-Ejhieh, Increased photocatalytic activity of Zn (II)/Cu (II) oxides and sulfides by coupling and supporting them onto clinoptilolite nanoparticles in the degradation of benzophenone aqueous solution, J. Hazard. Mater. 316 (2016) 194–203.
[39] J.O. Tijani, O.O. Fatoba, G. Madzivire, L.F. Petrik, A review of combined advanced oxidation technologies for the removal of organic pollutants from water, Water Air, Soil Pollut. 225 (9) (2014) 2102.
[40] K. Rusevova, F.-D. Kopinke, A. Georgi, Nano-sized magnetic iron oxides as catalysts for heterogeneous Fenton-like reactions—Influence of Fe (II)/Fe (III) ratio on catalytic performance, J. Hazard. Mater. 241 (2012) 433–440.
[41] G. Li Puma, P.L. Yue, Effect of the radiation wavelength on the rate of photocatalytic oxidation of organic pollutants, Ind. Eng. Chem. Res. 41 (23) (2002) 5594–5600.
[42] R.D.C. Soltani, S. Jorfi, H. Ramezani, S. Purfadakari, Ultrasonically induced ZnO–biosilica nanocomposite for degradation of a textile dye in aqueous phase, Ultrason. Sonochem. 28 (2016) 69–78.
[43] J. Chandrapala, C.M. Oliver, S. Kentish, M. Ashokkumar, Use of power ultrasound to improve extraction and modify phase transitions in food processing, Food Rev. Int. 29 (1) (2013) 67–91.
[44] M. Auta, B. Hameed, Chitosan–clay composite as highly effective and low-cost adsorbent for batch and fixed-bed adsorption of methylene blue, Chem. Eng. J. 237 (2014) 352–361.
[45] D. Tang, G. Zhang, Ultrasonic-assistant fabrication of cocoon-like Ag/$AgFeO_2$ nanocatalyst with excellent plasmon enhanced visible-light photocatalytic activity, Ultrason. Sonochem. 37 (2017) 208–215.
[46] M. Pelaez, P. Falaras, V. Likodimos, K. O'Shea, A. Armah, P.S. Dunlop, J.A. Byrne, D.D. Dionysiou, Use of selected scavengers for the determination of NF-TiO_2 reactive oxygen species during the degradation of microcystin-LR under visible light irradiation, J. Mol. Catal. A: Chem. 425 (2016) 183–189.
[47] Y. Liu, Y. Zhang, H. Guo, X. Cheng, H. Liu, W. Tang, Persulfate-assisted photodegradation of diethylstilbestrol using monoclinic $BiVO_4$ under visible-light irradiation, Environ. Sci. Pollut. Res. 24 (4) (2017) 3739–3747.
[48] H.N. McQuaid, M.F. Muir, L.E. Taggart, S.J. McMahon, J.A. Coulter, W.B. Hyland, S. Jain, K.T. Butterworth, G. Schettino, K.M. Prise, Imaging and radiation effects of gold nanoparticles in tumour cells, Scientific Rep. 6 (2016) 19442.
[49] V.K. Gupta, S. Kumar, R. Singh, L.P. Singh, S.K. Shoora, B. Sethi, Cadmium (II) ion sensing through p-tert-butyl calix[6]arene based potentiometric sensor, J. Mol. Liq. 195 (2014) 65–68.
[50] S. Karthikeyan, V.K. Gupta, R. Boopathy, A. Titus, G. Sekaran, A new approach for the degradation of aniline by mesoporous activated carbon as a heterogeneous catalyst: kinetic and spectroscopic studies, J. Mol. Liquids 173 (2012) 153–163.
[51] V.K. Gupta, A.K. Singh, L.K. Kumawat, Thiazole Schiff base turn-on fluorescent chemosensor for Al^{3+} Ion, Sens. Actuat.: B. Chem. 195 (2014) 98–108.
[52] T.A. Saleh, V.K. Gupta, Synthesis and characterization of alumina nano-particles polyamide membrane with enhanced flux rejection performance, Sep. Purf. Technol. 89 (2012) 245–251.
[53] N. Mohammadi, H. Khani, Shilpi Agarwal, V.K. Gupta, Adsorption process of methyl orange dye onto mesoporous carbon material- kinetic and thermodynamic studies, J. Colloids Interface Sci. (2011) 457–462.
[54] V.K. Gupta, B. Sethi, R.A. Sharma, Shilpi Agarwal, Arvind Bharti, Mercury selective potentiometric sensor based on low rim functionalized thiacalix [4] arene as a cationic receptor, J. Mol. Liq. 177 2013 114–118.
[55] T.A. Saleh, V.K. Gupta, Processing methods and characteristics of porous carbons derived from waste rubber tires: a review, Adv. Colloid Interface Sci. 211 (2014) 92–100.
[56] Tawfik A. Saleh, Shilpi Agarwal, V.K. Gupta, Synthesis of MWCNT/MnO_2 composites and their application for simultaneous oxidation of arsenite and sorption of arsenate, Appl. Catal. B: Env. 106 (2011) 46–53.
[57] V.K. Gupta, A. Nayak, S. Agarwal, Bioadsorbents for remediation of heavy metals: current status and their future prospects, Environ. Eng. Res. 20 (1) (2015) 001–018.
[58] V.K. Gupta, M.R. Ganjali, P. Norouzi, H. Khani, A. Nayak, Shilpi Agarwal, Electrochemical analysis of some toxic metals and drugs by ion selective electrodes, Crit. Rev. Anal. Chem. 41 (2011) 282–313.
[59] V.K. Gupta, Necip Atar, M.L. Yola, Zafer Üstündağ, Lokman Uzun, A novel magnetic Fe@Au core-shell nanoparticles anchored graphene oxide recyclable nanocatalyst for the reduction of nitrophenol compounds, Water Res. 48 2014 210–217.
[60] N. Mohammadi, H. Khani, Shilpi Agarwal, V.K. Gupta, Adsorption process of methyl orange dye onto mesoporous carbon material- kinetic and thermodynamic studies, J. Colloids Interface Sci. 362 (2011) 457–462.
[61] S.K. Srivastava, V.K. Gupta, M.K. Dwivedi, S. Jain, Anal. Proc. Anal. Commun. 32 (1995) 21–23.
[62] S.K. Srivastava, V.K. Gupta, S. Jain, Analyst 120 (1995) 495–498.